ELSEVIER

Coordination Chemistry Reviews
182 (1999) 125–173

COORDINATION CHEMISTRY REVIEWS

Alkylcycloarsoxanes and alkylcycloarsathianes—ambidentate macrocyclic ligands of variable metal-mediated ring size

William S. Sheldrick *, Iris M. Müller

Lehrstuhl für Analytische Chemie, Ruhr-Universität Bochum, D-44780 Bochum, Germany

Received 13 March 1998; accepted 17 July 1998

Contents

* Corresponding author. Tel.: +49-234-7004192; Fax: +49-234-7094420; e-mail: shel@anachem.ruhr-uni-bochum.de.

PII: S0010-8545(98)00195-7

Abstract

A comprehensive account of the coordination chemistry of alkylcycloarsoxanes $(RAsO)_n$ and alkylcycloarsathianes $(RAsS)_n$ is presented. The former ambi- and multidentate ligands are characterised by their unique ability to undergo metal-mediated ring expansion to $n = 5,6$ or 8. Cyclotetramers, -pentamers and hexamers of their sulphur analogues have also been stabilised as intact species in metal coordination spheres. At elevated temperatures As–S bond cleavage and metal-assisted reassembly afford novel linear and macrocyclic As–S ligands. Cyclotetramers $(RAsO)_4$ can be employed for the self-assembly of copper(I) halide based porous lamellar and framework coordination polymers capable of hosting alkali cations or polar molecules as guests.

Keywords: Alkylcycloarsoxanes; Alkylcycloarsathianes; Ambidentate; Macrocyclic; Ring expansion

1. Introduction

Although 140 years have now passed since $(CH_3AsO)_n$ and $(CH_3AsS)_n$ were first reported by von Baeyer [1], it is only in recent years that their potential as ambidentate macrocyclic ligands has been recognised and explored. In his original publication "Über die Verbindungen des Arsens mit dem Methyle", in which he prepared methylcycloarsoxane by alkaline hydrolysis of CH_3AsCl_2 and methylcycloarsathiane by passing H_2S through an aqueous solution of the same compound, von Baeyer assumed that both products must be present in a monomeric form. Reports on the analogous phenyl derivatives $(PhAsO)_n$ [2] and $(PhAsS)_n$ [3] appeared in German journals in the period 1877–1882. Despite considerable interest in the fungicidal and bactericidal properties of cycloarsoxanes $(RAsO)_n$ in the early 1920s [4], it was only in 1930 that Blicke and Smith [5] were able to confirm the oligomeric nature of this class of compounds. Their ebullioscopic and cryoscopic measurement suggested that cyclotetramers predominate for both $(PhAsO)_n$ and $(PhAsS)_n$ in CCl_4 or camphor solution.

In contrast, ^{1}H-NMR studies [6,7] have demonstrated that $(CH_3AsO)_n$ is present as a mixture of dimeric, trimeric, tetrameric and pentameric forms in benzene or CCl_4 solution. It is apparent from Fig. 1 that cyclotrimers and cyclotetramers provide the major species. Our own ^{1}H-NMR investigations [8] have confirmed the presence of analogous dynamic reorganisation equilibria between oligomeric forms of $(C_2H_5AsO)_n$ in chloroform. However, ebullioscopic measurements by Durand and Laurent [7] indicate that the average nuclearity n for alkylcycloarsoxanes $(RAsO)_n$ in benzene solution decreases from 3.6 for $R = CH_3$ to 2.9–3.1 for the longer alkyl side-chains $R = C_2H_5$, n-C_3H_7, n-C_4H_9. Preferred crystallisation of the

predominate cyclotetramers has been observed in those three cases for which an X-ray structural analysis has been performed on an organylcycloarsoxane (R = CH_3 [9], Ph [10], mesityl [11]).

Analogous eight-membered $(AsS)_4$ rings have also been established for a series of organylcycloarsathianes $(RAsS)_n$, R = C_2H_5 [12], *t*-C_4H_9 [13], Ph [14], in the solid state. Cryoscopic and ebullioscopic molecular weight measurements [15–17] suggest that cyclotrimers and cyclotetramers once again provide the major species in organic solvents. In the case of $(CH_3AsS)_n$, it has proved possible to coprecipitate both cyclooligomers as distinct crystalline forms from a CH_2Cl_2 solution [18]. Furthermore $(CH_3AsS)_3$ and $(CH_3AsS)_4$ could also be successfully separated by column chromatography with alumina as the stationary phase [18]. The presence of two major sets of resonances for the CH_2 and CH_3 protons of ethylcycloarsathiane in a chloroform solution (Fig. 2) is likewise in accordance with a dynamic equilibrium between the cyclotrimer and cyclotetramer [12].

Both $(RAsO)_n$ and $(RAsS)_n$ are potentially ambi- and multidentate macrocyclic ligands. The presence of competing sets of alternating soft As and hard O donor atoms in the organylcycloarsoxanes and their low energy barriers to ring contraction or expansion in organic solvents suggest that this class of compounds should exhibit a rich variety of binding modes. The structural similarity of $(RAsO)_n$ and $(RAsS)_n$ to ion ligating crown ethers and crown thioethers is particularly intriguing. It is, therefore, somewhat surprising to note that the first example of a metal complex of such a ligand was reported only in 1986, namely [{$Mo(CO)_3$}$_2${*cyclo*-$(CH_3AsO)_6$}], which was serendipitously assembled by Rheingold and DiMaio [19] by reacting $Mo(CO)_6$ with *cyclo*-$(CH_3As)_5$ in toluene in the presence of a stoichiometric quantity of O_2 in a Carius tube at 150°C. The thereby documented ability of $(CH_3AsO)_n$ to undergo metal-mediated ring expansion has been found to be characteristic for all organylcycloarsoxanes investigated in our group (R = CH_3, C_2H_5, Ph). We have also discovered that the cyclotetramers $(CH_3AsO)_4$ and $(C_2H_5AsO)_4$ can be employed as bridging ionophoric spacer molecules for the construction of a variety of flexible lamellar and framework coordination polymers, whose cavities are capable of imbibing molecular guests. The present review

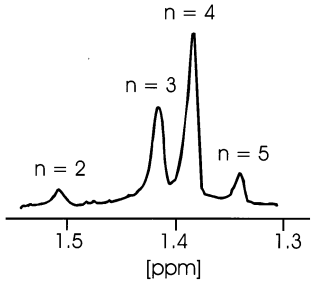

Fig. 1. ^{1}H-NMR spectrum (60 MHz) of a CCl_4 solution of $(CH_3AsO)_n$ with the assignment of individual resonances to cyclic oligomers of nuclearity n [7].

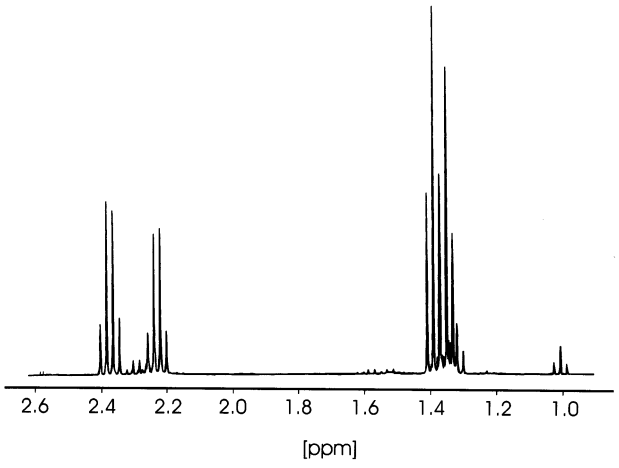

Fig. 2. ^{1}H-NMR spectrum (400 MHz) of a $CDCl_3$ solution of $(CH_3AsS)_n$ [12].

provides a comprehensive account of the coordination chemistry of these fascinating macrocyclic ligands.

2. Coordination chemistry of organylcycloarsoxanes

2.1. Preparation and structure of $(RAsO)_n$

The preparation and properties of organylcycloarsoxanes $(RAsO)_n$ were discussed in detail by Tzschach and Heinicke in their 1978 book on arsenic heterocycles [20] and more briefly by Sowerby in a later monograph on inorganic homo- and heterocycles [21]. Several methods are available for the synthesis of these colourless solids: (a) treatment of a benzene solution of $RAsX_2$ (X = Cl, Br, I) with Na_2CO_3 or K_2CO_3 and a trace of water [22,23], (b) reduction of arsonic acids (usually with SO_2/HCl) followed by alkaline hydrolysis [24,25], and (c) oxidation of primary arsines or cyclopolyarsines $(RAs)_n$ [26,27]. As von Baeyer mentioned in his original report on methylcycloarsoxane [1], after removal of organic solvents from the resulting cyclooligomers $(RAsO)_n$, the presence of small quantities of impurities often leaves viscous oils, which subsequently solidify to glassy products. Although von Baeyer described the successful crystallisation of $(CH_3AsO)_n$ after purification ("würfelförmige Krystalle"), it was only in 1991 that DiMaio and Rheingold were able to structurally characterise a cyclooligomer of methylcycloarsoxane by successfully isolating $(CH_3AsO)_4$ as a crystalline solid from the aerobic oxidation of *cyclo*-$(CH_3As)_5$ in the presence of $Mn_2(CO)_{10}$, with the latter transition metal carbonyl serving presumably as the source of a metal template [9]. This cyclotetramer exhibits the boat-chair conformation (Fig. 3) that is energetically favoured

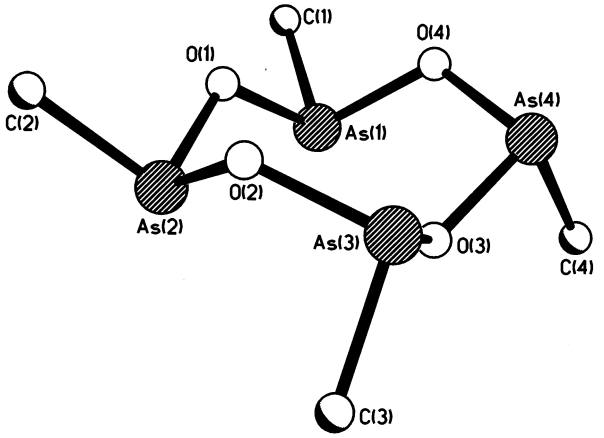

Fig. 3. Boat-chair conformation of the cyclotetramer $(CH_3AsO)_4$ in the solid state [9]. Endocyclic torsion angles beginning at As(1)–O(1) are as follows: −109.6, 101.4, −89.2, 33.4, 102.3, −109.2, −24.7, 92.5°.

for isolobal cyclooctane [28]. All four organyl substituents occupy equatorial sites in $(CH_3AsO)_4$ as they also do in $(PhAsO)_4$ with its analogous boat-chair conformation [10] and $(mesAsO)_4$ (mes = mesityl), which adopts the somewhat less favourable crown conformation (Fig. 4) in the solid state [11]. This implied conformational flexibility has likewise been established for bridging cyclotetramers $(RAsO)_4$ ($R = CH_3$, C_2H_5) in coordination polymers (Section 2.3), for which a third variant, the twist-chair conformation is often employed. As–O distances in the cyclotetramers fall within a narrow range (1.770–1.819 Å) and average to respectively 1.792 ($R = CH_3$), 1.796 (R = Ph) and 1.790 Å (R = mes), values similar to that of 1.80 Å in the As_4O_6 cage [29]. Although the endocyclic As–O–As angles in $(RAsO)_4$ are still relatively wide in comparison to an idealised tetrahedral value, it

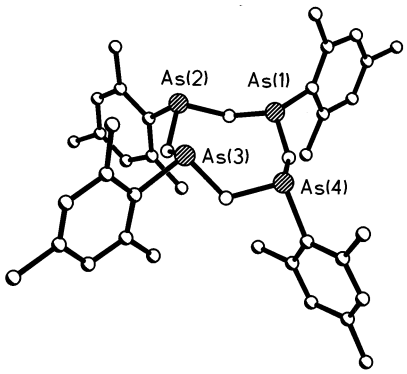

Fig. 4. Crown conformation of the cyclotetramer $(mesAsO)_4$ in the solid state [11]. Endocyclic torsion angles beginning at As(1)–O(1) are as follows: 92.1, −81.7, 85.8, −112.5, 110.7, −81.9, 75.7, −88.5°.

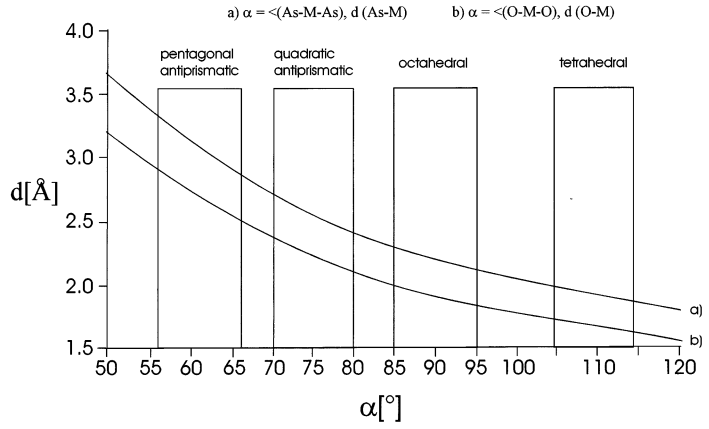

Fig. 5. Dependence of As–M–As (M = metal atom) and O–M–O angles, respectively, on (a) As–M or (b) O–M distances in four-membered chelate rings. The following typical values were employed: d(As–O) = 1.80 Å, d(As^{M}–O) = 1.78 Å, ∠(As–O–As) = 121.8°, ∠(O–As–O) = 96° with As^{M} standing for coordinating arsenic atoms.

is interesting to note that their average sizes of 121.7 (R = CH_3), 120.2 (R = Ph) and 117.3° (R = mes) are appreciably smaller than those of 126 and 129° in the supported arsoxane rings of $(CH_2)_3As_4O_4(CH_2)_3$ [30] and $As_4O_4(CH_2)_2$ [31].

2.2. Metal-mediated ring expansion

2.2.1. Conformational aspects

As discussed in Section 1, ^{1}H-NMR investigations have indicated that the alkylcycloarsoxanes $(CH_3AsO)_n$ and $(C_2H_5AsO)_n$ are present in organic solvents as a mixture of cyclic oligomers, of which cyclotrimers and cyclotetramers predominate [7,8]. Taking the low associated energy barriers into account, metal templates should be capable of mediating ring size reorganisation to enable optimal occupation of vacant sites in the metal coordination sphere by suitable donor atoms of a cyclooligomer. The nuclearity n of the organylcycloarsoxane ligands $(RAsO)_n$ should be such as to favour the adoption of an energetically preferred conformation in the resulting metal complex. Simple geometrical considerations allow the following general predications:

1. $\kappa^2 As^1,As^2$ chelation by adjacent arsenic atoms should be possible in octahedral but not in tetrahedral transition metal coordination spheres.
2. $\kappa^2 O^1,O^2$ chelation by adjacent oxygen atoms should be possible in tetragonal and pentagonal antiprismatic alkali cation coordination spheres.Using average As–O distances and As–O–As angles for alkylcycloarsoxane complexes, Fig. 5 depicts the dependence of the As–M–As and O–M–O angles in hypothetical four membered chelate rings on the As–M or O–M distances involved. Characteristic angle ranges for tetrahedral, octahedral, tetragonal and pentagonal antiprismatic coordination spheres are indicated. $\kappa^2 As^1,As^2$ chelation can be

ruled out for a tetrahedral coordination sphere, in view of the fact that the required As–M distances would be much shorter than typical values of 2.25–2.55 Å for transition metals.

3. Cyclotetramers $(RAsO)_4$ should be expected to prefer the boat-chair or crown conformations when bridging adjacent metal atoms in the μ-1κAs^1:2κAs^2 mode but the energetically less favourable twist-chair conformation when connecting bulky metal fragments in the μ-1κAs^1:2κAs^3 coordination mode.The three ring conformations found for $(RAsO)_4$ in metal complexes are depicted in Fig. 6. It is apparent that the twist-chair conformation allows a maximisation of the distance between metal centres coordinated to opposite arsenic atoms As^1 and As^3 and is, therefore, well-suited for the construction of supramolecular structures.
4. Facial coordination of a transition metal fragment can best be achieved by the $\kappa^3 As^1, As^3, As^5$ mode of a cyclohexamer $(RAsO)_6$.The directions of the arsenic non-bonded electron pairs are depicted in Fig. 7 for both a cyclotrimer and a cyclohexamer. Whereas the cuboctahedral conformation of $(RAsO)_6$ should be capable of coordinating a metal fragment such as $M(CO)_3$ with a minimum of conformational change, severe ring strain would clearly be introduced in the case of $(RAsO)_3$.
5. Fourfold equatorial coordination of a transition metal can best be achieved by the $\kappa^4 As^1, As^3, As^5, As^7$ mode of a cyclooctamer $(RAsO)_8$. Extension of the arguments presented for a facial coordination lead to the prediction that

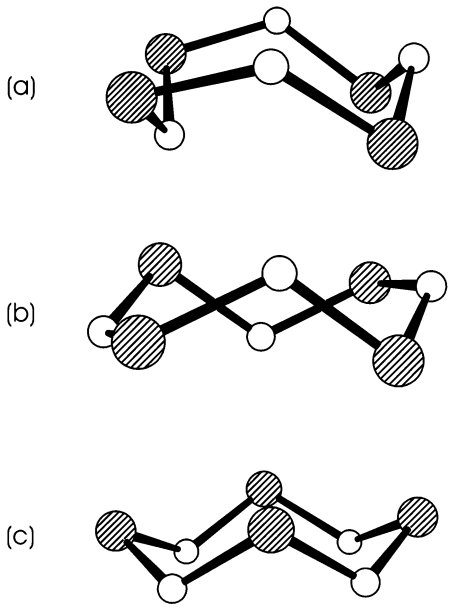

Fig. 6. (a) Boat-chair, (b) twist-chair and (c) crown conformations of the $(AsO)_4$ ring in cyclotetramers $(RAsO)_4$.

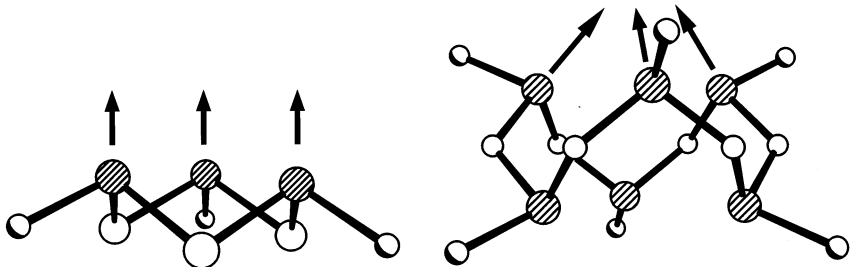

Fig. 7. Directions of lone pairs available for As–M coordination by methylcycloarsoxane: (a) as a cyclotrimer in its preferred chair conformation, (b) as a cyclohexamer with a flattened cuboctahedral conformation.

fourfold equatorial coordination should enable the stabilisation of cyclooctamers $(RAsO)_8$ previously undetected in solutions of organylcycloarsoxanes.

2.2.2. $\kappa^n O$ coordination ($n = 4$, 5)

Both $(CH_3AsO)_n$ and $(C_2H_5AsO)_n$ are capable of acting as ionophores for alkali cations in a manner similar to classical crown ethers, and the ring size in their sandwich complexes $[M\{cyclo\text{-}(RAsO)_n\}_2]SCN$ ($M = Na$, $n = 4$; $M = K$, $n = 5$) [32,33] is clearly controlled by the radius of the central cation (Fig. 8). Although analogous complexes have not been crystallised for Rb^+ or Cs^+, $^1_\infty[\{Cs[cyclo\text{-}(C_2H_5AsO)_5]_2\}Cu_2(\mu\text{-}I)I_2]$ [34], which may be prepared by self-organisation from CsI, CuI and $(C_2H_5AsO)_n$ in acetonitrile, contains $[Cs\{cyclo\text{-}(C_2H_5AsO)_5\}_2]^+$ sandwich cations, that are linked through $1\kappa As^1{:}2\kappa As^2$-coordinated $[Cu_2I_3]^-$ anionic units into polymeric *zweier* single chains (Fig. 9). A pentagonal antiprismatic arrangement of two cyclopentamers has also been established for $[(NH_4)\{cyclo\text{-}(C_2H_5AsO)_5\}_2][Ag(SCN)_2]$ [34]. As no significant metrical differences are observed for alkali cation coordination by either $(CH_3AsO)_n$ or $(C_2H_5AsO)_n$ ($n = 4$, 5) and

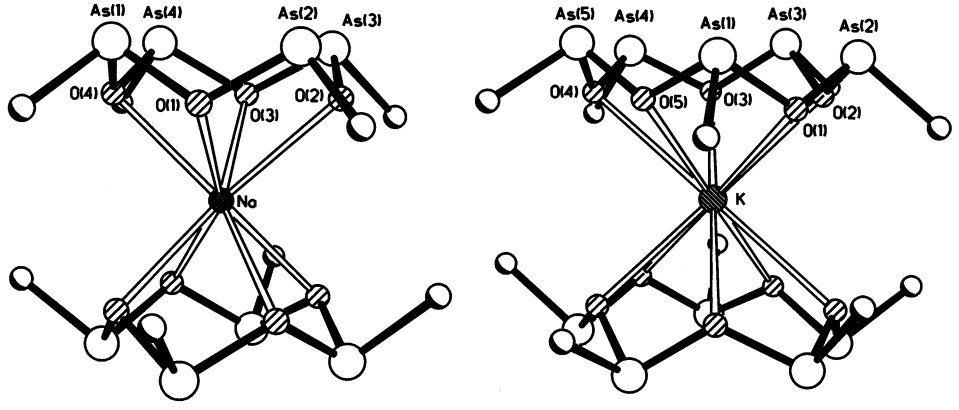

Fig. 8. Sandwich cations of $[Na\{cyclo\text{-}(CH_3AsO)_4\}_2]SCN$ and $[K\{cyclo\text{-}(CH_3AsO)_5\}_2]SCN$ [32].

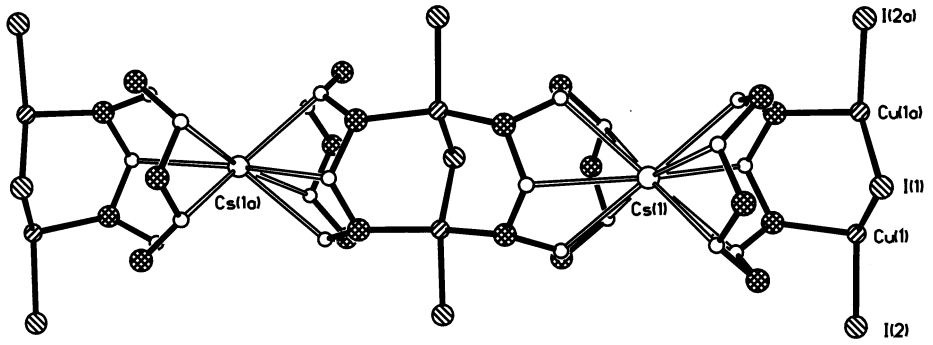

Fig. 9. *Zweier* single chain of $^{1}_{\infty}[\{Cs[cyclo\text{-}(C_2H_5AsO)_5]_2\}Cu_2(\mu\text{-}I)I_2]$ with pentagonal antiprismatic coordination of the participating Cs^+ cations [34].

more examples are known for the latter alkylcycloarsoxane, discussion of structural details will be restricted to this cyclic ionophore. Based on the typical O···O distance of 2.68 Å between adjacent oxygen atoms and tabulated values of alkali cation radii (Shannon and Prewitt [35]), Table 1 lists expected values for the distance M···Pl where Pl marks the centre of the O_n plane of an undistorted crown-shaped $\kappa^n O$ coordinating alkylcycloarsoxane. The good agreement between observed and predicted values for $[Na\{cyclo\text{-}(C_2H_5AsO)_4\}_2]^+$ and $[K\{cyclo\text{-}(C_2H_5AsO)_5\}_2]^+$ confirms that the respective undistorted cyclooligomers provide a satisfactory pore size for the alkali cation involved. Although the results suggest that the Cs^+ cation is rather too large to stabilise a cyclopentamer $(C_2H_5AsO)_5$ in an isolated sandwich cation, they also indicate that the alternative 12-fold coordination by a crown-shaped cyclohexamer would lead to a very unfavourable squashed

Table 1
Expected values for undistorted crown-shaped ethylcycloarsoxanes and averaged experimental bond length (Å) and angles (°) in sandwich cations $[M\{cyclo\text{-}(C_2H_5AsO)_n\}_2]^+$

n	Cation	*d*(O···O)	*d*(M–O) [35]	*d*(M···Pl)	∠(O–M–Pl)	∠(O–M–O)
Expected values						
3	Li^+	2.68	2.14	1.48	46.2	77.5
4	Na^+	2.68	2.56	1.72	47.8	63.1
4	K^+	2.68	2.91	2.20	40.9	54.8
5	K^+	2.68	2.99	1.93	49.8	53.3
5	Rb^+	2.68	3.00	1.95	49.5	53.1
5	Cs^+	2.68	3.21	2.26	45.2	49.3
6	Cs^+	2.68	3.28	1.89	54.8	48.2
Observed values						
4	Na^+	2.69	2.59	1.76	47	62.4
5	K^+	2.68	2.99	1.92	50	53.4
5	NH_4^+	2.69	3.01	1.96	49	53.1
5	Cs^+	2.69	3.26	2.33	45	48.5

hexagonal antiprismatic geometry with d(Cs···Pl) even shorter than in [K{*cyclo*-$(C_2H_5AsO)_5$}$_2$]$^+$. On the basis of Table 1, Li^+ cations might also be expected to be capable of stabilising cyclotrimers in sandwich cations of the type [Li{*cyclo*-$(RAsO)_3$}$_2$]$^+$.

It is interesting to compare the coordination geometries of [Na{*cyclo*-$(C_2H_5AsO)_4$}$_2$]$^+$ and [K{*cyclo*-$(C_2H_5AsO)_5$}$_2$]$^+$ with those found in the analogous crown ether complexes [Na(12-crown-4)$_2$]OH·8H_2O [36] and [K(benzo-15-crown-5)$_2$]I [37]. On the basis of a simple ionic model, Kepert has determined an O–M–Pl angle (α) of 59.3° for an idealised quadratic antiprism, but typical experimental values are found to be somewhat smaller (57°) in the complexes ML_8 of monodentate ligands [38]. [Na{*cyclo*-$(C_2H_5AsO)_4$}$_2$]$^+$ exhibits a very small average α angle of 47.2°, [Na(12-crown-4)$_2$]$^+$ a larger value of 52.6°. The extreme degree of elongation of the quadratic antiprism in the $(C_2H_5AsO)_4$ sandwich cation results from the shortness of the O···O distance (2.69Å) in the cyclotetramer in comparison to the more flexible crown ether (2.80 Å). The better ion ligating properties of 12-crown-4 are also confirmed by its average Na···O distances, which are some 0.10 Å shorter than in [Na{*cyclo*-$(C_2H_5AsO)_4$}$_2$]$^+$. A similar trend is apparent for [K{*cyclo*-$(C_2H_5AsO)_5$}$_2$]$^+$ ($\alpha = 50°$, d(K···O) = 2.99 Å) and in [K(benzo-15-crown-5)$_2$]$^+$ ($\alpha = 54°$, d(K···O) = 2.86 Å). Both α values are markedly smaller than that of 59.8° calculated by Kepert for an idealised pentagonal antiprism and solution studies confirm the relatively poor ionophoric properties of alkylcycloarsoxanes. On redissolving [Na{*cyclo*-$(RAsO)_4$}$_2$]SCN or [K{*cyclo*-$(RAsO)_5$}$_2$]SCN, ^{1}H-NMR spectra are in accordance with a distribution of cyclooligomers ($n = 2–5$) similar to that found for $(RAsO)_n$ alone [7,8,32].

2.2.3. κ^nAs coordination

2.2.3.1. Cyclotetramers and cyclopentamers $(RAsO)_n$ ($n = 4$, 5). Cyclotetramers $(RAsO)_4$ and cyclopentamers $(RAsO)_5$ adopt a bridging role in all their previously characterised metal complexes. The vast majority of these are coordination polymers and will, therefore, be classified in detail in Section 2.3. Characteristic for the $(AsO)_4$ eight membered ring in alkylcycloarsoxanes ($R = CH_3$, C_2H_5) is its remarkable flexibility, which allows it to bridge between two and four metal atoms. Known coordination modes for the three preferred ring conformations, boat-chair (bc), twist-chair (tc) and crown (cr) (Fig. 6) are depicted in a schematic manner in Fig. 10. Representative examples will now be considered.

2.2.3.1.1. Twist-chair conformation (tc13, tc4). The tc13 mode, which is particularly suitable for connecting bulky metal fragments, has been observed in both discrete and polymeric coordination compounds. For instance, two $MnCp'(CO)_2$ units ($Cp' = CH_3C_5H_4$) are linked in this manner in [{$MnCp'(CO)_2$}{μ-*cyclo*-$(CH_3AsO)_4$}], that may be synthesised either by treatment of [$MnCp'(CO)_3$] with *cyclo*-$(CH_3AsO)_5$ in the presence of air or by direct reaction of the transition metal carbonyl with $(CH_3AsO)_n$ [9]. An analogous bridging role is found in the cyclic oligomer [*cyclo*-{$ReBr(CO)_3$[μ-{*cyclo*-$(C_2H_5AsO)_4$}]}$_4$] (Fig. 11), prepared by reacting [$ReBr(CO)_5$] with $(C_2H_5AsO)_n$ in refluxing toluene [34]. As–O bonds to

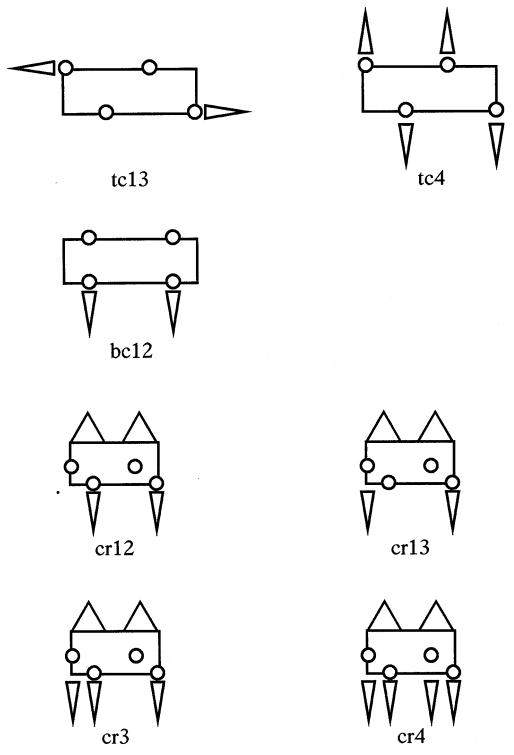

Fig. 10. Schematic representations of $(RAsO)_4$ bridging modes: tc13 = μ:1κAs^1:2κAs^3 twist-chair; tc4 = μ_4:1κAs^1:2κAs^2:3κAs^3:4κAs^4 twist-chair; bc12 = μ:1κAs^1:2κAs^2 boat-chair; cr12 = μ-1κAs^1:2κAs^2 crown; cr13 = μ-1κAs^1:2κAs^3 crown; cr3 = μ_3-1κAs^1:2κAs^2:3κAs^3 crown; cr4 = μ_4-1κAs^1:2κAs^2:3κAs^3:4κAs^4 crown.

coordinated arsenic atoms in this complex exhibit an average value of 1.754(8) Å in comparison to 1.819(7) Å for non-coordinated As atoms, a change accompanied by a concomitant widening of the average O–As–O angles from 95(1) to 103(1)°. Alkylcycloarsoxanes might be expected to be relatively weak π-acceptors and this prognosis is confirmed in the tetrameric Re complex by the registration of an increased degree of π-backbonding to the CO ligands in *trans* position to the coordinated As atoms. The relevant carbonyl IR absorption bands are shifted to lower wavenumbers (2055, 1929 cm^{-1}) in comparison to $[ReBr(CO)_5]$ (2150, 2044 cm^{-1}) [39].

Examples of the tc4 mode are found in copper halide-rich networks of the type $[Cu_nX_n\{cyclo\text{-}(CH_3AsO)_4\}_2]$ ($n = 3$, 4, 6) [40,41]. For instance infinite $^1_\infty[CuX]$ (X = Br, I) single chains are linked by methylcycloarsoxane ligands in a twist-chair conformation (Fig. 12) through all four As atoms into sheets $^2_\infty[\{CuX(CuX{\cdot}CH_3CN)_2\}\{cyclo\text{-}(CH_3AsO)_4\}]$.

2.2.3.1.2. Boat-chair conformation (bc12). Although the energetically favourable boat-chair conformation has been established for both $(CH_3AsO)_4$ [9] and $(PhAsO)_4$ [10] in the solid state, only one example is known for a metal complex. Two adjacent

copper atoms Cu(3) and Cu(4) in the chain coordination polymer $^{1}_{\infty}[Cu_4Cl_4\{cyclo\text{-}(C_2H_5AsO)_4\}_3]$ [42] are bridged in the bc12 mode by an ethylcycloarsoxane tetramer of approximately C_S symmetry (Fig. 13). Interestingly this complex also contains further $(C_2H_5AsO)_4$ ligands with contrasting tc13 [As13, As1b and As24, As2a] and cr4 [As12–As42] bridging functions.

2.2.3.1.3. Crown conformation (cr12, cr13, cr3, cr4). Although tc13 and tc4 bridging roles are more typical for alkylcycloarsoxanes, the coordination requirements of the alkali countercation lead to the adoption of the unusual cr12 and cr13 modes in the anionic ribbons of $[Cs(H_2O)_2][Cu_3I_4\{cyclo\text{-}(CH_3AsO)_4\}_2]\cdot 0.5CH_3OH$ [43]. A further optimisation of the multidentate ligand properties of $(CH_3AsO)_4$ is achieved in $^{3}_{\infty}[\{Cs[cyclo\text{-}(CH_3AsO)_4]Cu_3I_4\}\{cyclo\text{-}(CH_3AsO)_4\}]$ [32], in which the heterocycle now coordinates not only a Cs^+ cation in a crown κ^4O fashion but also three I-bridged Cu(I) atoms through three of its four available As atoms in the cr3 mode. As may be seen in Fig. 14, the iodine atoms of a translation-related Cu_3I_4 unit complete the 8-fold approximately cube-like coordination sphere of the alkali cation as a horseshoe part of an incomplete Cu_4I_4 crown.

A crown-shaped As_4O_4 ring coordinated in a cr3 or cr4 manner to three or four Cu(I) atoms has been observed as a characteristic molecular building block in the polymeric $(C_2H_5AsO)_4$ complexes, $^{1}_{\infty}[Cu_4Cl_4\{cyclo\text{-}(C_2H_5AsO)_4\}_3]$ [42],

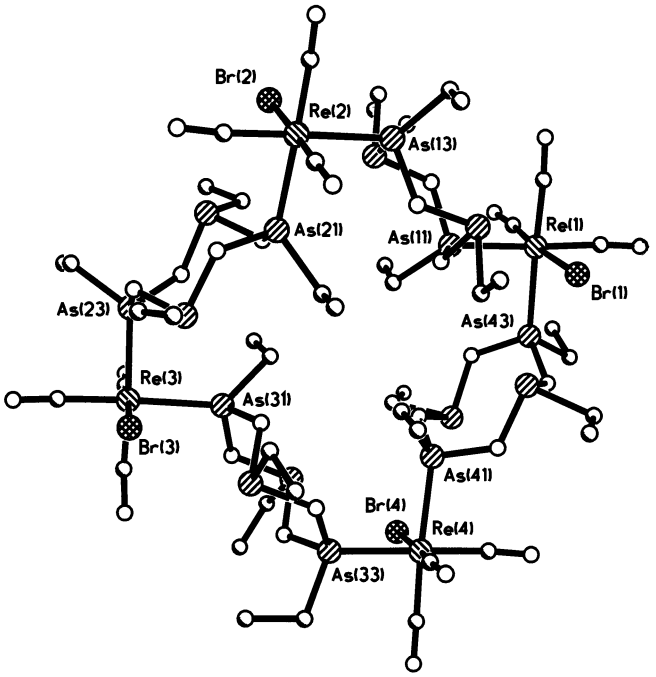

Fig. 11. Structure of the cyclic tetramer $[cyclo\text{-}\{ReBr(CO)_3[\mu\text{-}\{cyclo\text{-}(C_2H_5AsO)_4\}]\}_4]$ in which individual Re atoms are linked by $(C_2H_5AsO)_4$ ligands in the tc13 mode [34].

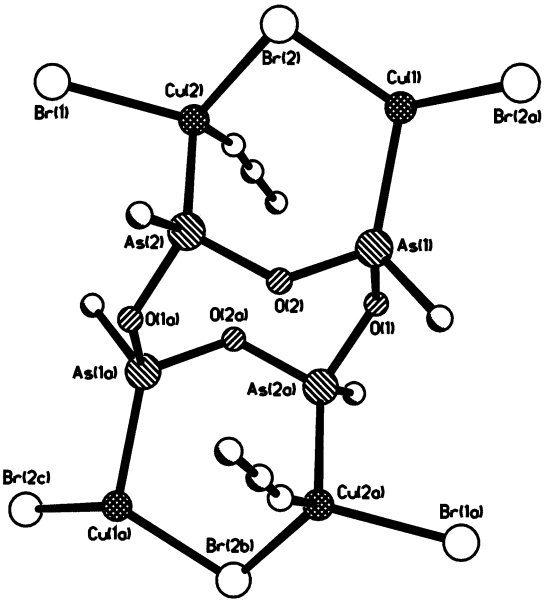

Fig. 12. tc4 bridging mode of the $(CH_3AsO)_4$ cyclotetramers in $^{2}_{\infty}[\{CuBr(CuBr{\cdot}CH_3CN)_2\}\{cyclo\text{-}(CH_3AsO)_4\}]$ [41].

$^{2}_{\infty}[Cu_3X_3\{cyclo\text{-}(C_2H_5AsO)_4\}_2]$ (X = Br [42], I [34]) and $^{2}_{\infty}[Cu_6I_6\{cyclo\text{-}(C_2H_5AsO)_4\}_3]$ [42]. All these examples contain a cr3 coordinated $[Cu_3(\mu_3\text{-}X)]^{2+}$ unit, that is extended by an additional $CuCl_2$ group to afford a six-membered Cu_3Cl_3 ring in the first of the coordination polymers. The cr4 coordination of all four Cu(I) atoms by the crown-shaped $(C_2H_5AsO)_4$ ligand [As12–As42] in this CuCl complex is depicted in Fig. 13.

The only known example of *κAs* coordination by a cyclopentamer $(RAsO)_5$ has already been mentioned in Section 2.2.2. A Cs^+ countercation is once again responsible for the stabilisation of crown-shaped heterocycles in $^{1}_{\infty}[\{Cs[cyclo\text{-}(C_2H_5AsO)_5]_2\}Cu_2(\mu\text{-}I)I_2]$ [34], in whose anionic partial structure, two cyclopentamers $(C_2H_5AsO)_5$ are linked through a $[Cu_2I_3]^-$ unit (Fig. 9).

2.2.3.2. Cyclohexamers $(RAsO)_6$. We have followed up Rheingold and DiMaio's original report on the indirect synthesis of $[\{Mo(CO)_3\}_2\{cyclo\text{-}(CH_3AsO)_6\}]$, through treatment of $Mo(CO)_6$ with *cyclo*-$(CH_3As)_5$ in toluene at 150°C in the presence of O_2 [19], by demonstrating that other cyclohexamers $(RAsO)_6$ (R = C_2H_5, Ph) can likewise be stabilised in the coordination sphere of facial transition metal carbonyl fragments $M(CO)_3$. However, in contrast to $[\{Mo(CO)_3\}_2\{cyclo\text{-}(CH_3AsO)_6\}]$ our series of analogous dinuclear Group 6 complexes $[\{M(CO)_3\}_2\{cyclo\text{-}(RAsO)_6\}]$ (R = C_2H_5, M = Cr, Mo, W [8]; R = Ph, M = Cr, Mo [10]) were all prepared by direct reaction of $M(CO)_6$ with $(RAsO)_n$ in toluene at 150–180°C. $[\{Cr(CO)_3\}_2\{cyclo\text{-}(C_2H_5AsO)_6\}]$ (**1**) is depicted as a representative example of this class of compounds in Fig. 15.

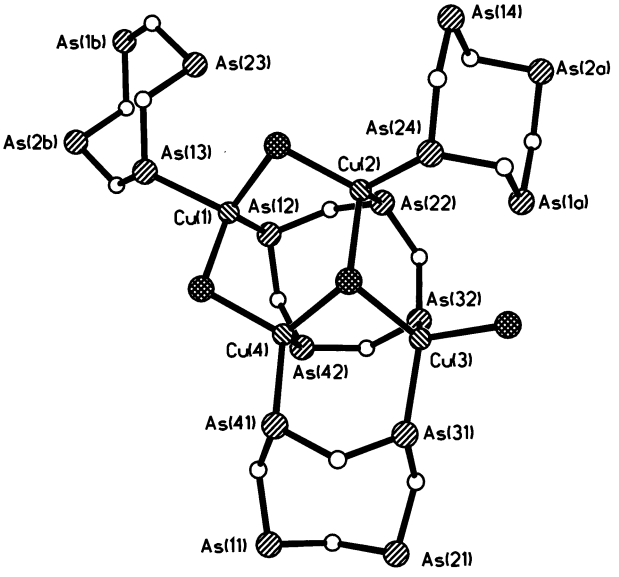

Fig. 13. The asymmetric unit of $^{1}_{\infty}[Cu_4Cl_4\{cyclo\text{-}(C_2H_5AsO)_4\}_3]$ with the three cyclotetramers $(C_2H_5AsO)_4$ of differing bridging mode: bc12 [As31, As41], tc13 [As24, As2a and As13, As1b] and cr4 [As12–As42]. Linkage to an infinite chain is through As(1b) and As(2a) [42].

As–O distances in the hexadentate cyclohexaarsoxane ligand in this complex lie in the range 1.784(5)–1.811(5) Å with an average value of 1.80(1) Å similar to that observed in $(RAsO)_4$ (R = CH_3, 1.792 Å [10]; R = mes, 1.790 Å [11]) and $[\{Mo(CO)_3\}_2\{cyclo\text{-}(CH_3AsO)_6\}]$ (1.791 Å [19]). A greater degree of flattening of

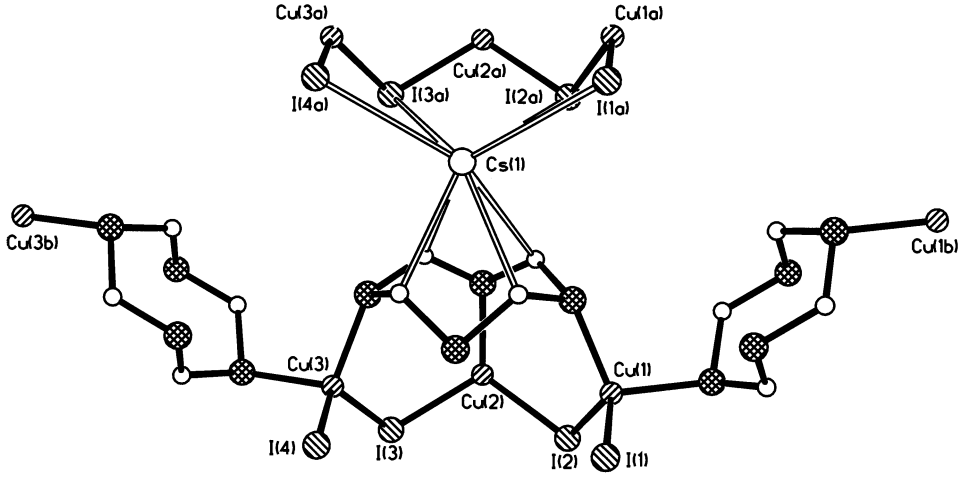

Fig. 14. Simultaneous crown κ^4O coordination of a Cs^+ cation and $1\kappa As^1{:}2\kappa As^2{:}3\kappa As^3$ coordination (cr3) of three Cu(I) atoms in $^{3}_{\infty}[\{Cs[cyclo\text{-}(CH_3AsO)_4]Cu_3I_4\}\{cyclo\text{-}(CH_3AsO)_4\}]$ [32].

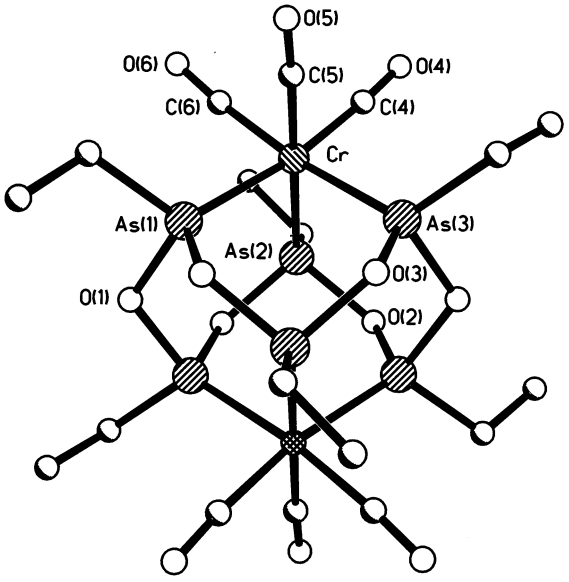

Fig. 15. Molecular structure of $[\{Cr(CO)_3\}_2\{cyclo\text{-}(C_2H_5AsO)_6\}]$ in which the twelve atoms of the As_6O_6 ring form a flattened cuboctahedron [8].

the As_6O_6 cuboctahedron is required to position the arsenic atoms for coordination of the smaller chromium atoms in comparison to the latter dimolybdenum complex. This is achieved by adoption of narrower As–O–As and O–As–O angles in the dichromium complex, where they lie in the respective ranges 115.3(3)–117.5(3)° and 98.5(2)–99.1(2)° in comparison to average values of 118.9 and 101.0° in $[\{Mo(CO)_3\}_2\{cyclo\text{-}(CH_3AsO)_6\}]$. In the chromium coordination sphere, C–Cr–C angles [84.3(4)–91.0(4)°] are significantly narrower than As–Cr–As angles [94.6(1)–95.7(1)°]. As a result of the much poorer π-acceptor properties of the hexaethylcyclohexaarsoxane ligand in $[\{Cr(CO)_3\}_2\{cyclo\text{-}(C_2H_5AsO)_6\}]$ in comparison to the CO ligands in $Cr(CO)_6$ [44], the Cr–C bond lengths in the first complex [1.857(8)–1.876(9) Å] are markedly shorter than in the hexacarbonyl, which exhibits an average value of 1.909 Å. The increased degree of π backbonding to the carbonyl ligands of the alkylcycloarsoxane complex is also reflected in the observed shifts of the ν(CO) frequencies from 2112, 2018 and 1986 cm^{-1} in the IR spectrum of $Cr(CO)_6$ to 1961 and 1898 cm^{-1} in $[\{Cr(CO)_3\}_2\{cyclo\text{-}(C_2H_5AsO)_6\}]$. CO stretching frequencies in similar ranges are also recorded for the analogous dimolybdenum (1970, 1920, 1904 cm^{-1}) and ditungsten (1962, 1908 cm^{-1}) complexes [8].

These findings prompted us to investigate the possible influence of M–As distances and As–M–As′ angles of a $\kappa^3 As$ facially coordinated metal atom on the nuclearity of $(RAsO)_n$ complexes. A metal mediated ring expansion of organylcycloarsoxanes to hexameric ligands $(RAsO)_6$ was observed for a series of complexes $[\{ReBr(CO)_2\}_2\{\mu\text{-}[cyclo\text{-}(C_2H_5AsO)_6\}]$ (**2**), $[RuCl_2\{cyclo\text{-}(C_2H_5AsO)_6\}(Ph_3P)]$ (**3**),

$[RhCl_3\{cyclo\text{-}(C_2H_5AsO)_6\}]$ (**4**), $[Cu_2\{\mu\text{-}[cyclo\text{-}(C_2H_5AsO)_6]\}\{(CH_3)_2PhP\}_2](CF_3SO_3)_2$ (**5**) [45] and $[\{RuCl_2(CO)\}_2\{\mu\text{-}[cyclo\text{-}(PhAsO)_6]\}]$ [10], despite differences in their nuclearity and metal coordination geometries. Average bond lengths and angles in **1–5** are summarised in Table 2.

As previously discussed in Section 2.2.3.1, reaction of ethylcycloarsoxane with $[ReBr(CO)_5]$ in refluxing toluene (110°C, 15 min) leads to substitution of only two carbonyl ligands and formation of the cyclic oligomer $[cyclo\text{-}\{ReBr(CO)_3[\mu\text{-}\{cyclo\text{-}(C_2H_5AsO)_4\}]\}_4]$ containing tetramers $(C_2H_5AsO)_4$ in their typical tc13 bridging mode [34]. At the higher temperature provided by refluxing mesitylene (165°C, 6 h), a further CO ligand may be replaced to enable the metal-assisted ring expansion of ethylcycloarsoxane to its hexameric form found in the dirhenium complex **2**. This compound is also isolated at the molar $[ReBr(CO)_5]$:$(C_2H_5AsO)_6$ ratio of 1:1 required for a mononuclear $\kappa^3As^1As^3As^5$ coordinated complex. In contrast to the preferred formation of a dinuclear complex for the facial $ReBr(CO)_2$ fragment, treatment of $(C_2H_5AsO)_n$ with either $[RuCl_2(Ph_3P)_3]$ or $RhCl_3{\cdot}3H_2O$ allows only the isolation of the mononuclear complexes **3** and **4** (Figs. 16 and 17). The *trans* influence of the Ph_3P ligand in **3** leads to a marked lengthening of the Ru1–As3 distance to 2.454(2) Å in comparison to the Ru1–As1 and Ru1–As5 distances of 2.372(2) and 2.354(2) Å. Increased strain in the As_6O_6 ring resulting from the presence of these short Ru–As distances causes the arsoxane ring to no longer adopt the flattened cuboctahedral conformation found in the dinuclear complexes **1** and **2** [torsion angles As′–O–As–O′ $\pm$(78.6) to $\pm$(81.4)° in **1**, $\pm$(76.2) to $\pm$(79.6)° in **2**]. The solid-state conformation of **3** depicted in Fig. 16 would be incapable of coordinating a second $RuCl_2(Ph_3P)$ fragment. Although the shape of the $(AsO)_6$ macrocycle in the mononuclear Rh(III) complex **4** does resemble a flattened cuboctahedron, the short Rh–As distances (2.34 Å) once again indicate a pronounced increase in ring strain, that may now be gauged from the striking difference between the average values for As′–O–As–O′ torsion angles when As is

Table 2
Average bond lengths (Å) and angles (°) in mono- and dinuclear complexes of $(C_2H_5AsO)_6$[a]

Compound	**1**	**2**	**3**	**4**	**5**
Metal fragment	$Cr(CO)_3$	$ReBr(CO)_2$	$RuCl_2(Ph_3P)$	$RhCl_3$	$Cu\{(CH_3)_2PhP\}$
Nuclearity	2	2	1	1	2
As–M	2.42(1)	2.49(5)	2.39(5)	2.34(1)	2.38(2)
As···As′	3.57(1)	3.67(1)	3.53(4)	3.57(2)	3.73(5)
As(M)–O	1.80(1)	1.79(1)	1.77(1)	1.75(1)	1.79(1)
As–O			1.80(1)	1.80(2)	
As–M–As′	95(1)	95(1)	95(1)	99(1)	103(1)
As–O–As′	116(1)	120(1)	121(3)	123(1)	120(1)
O–As(M)–O′	99(1)	100(2)	98(1)	102(2)	101(1)
O–As–O′			98(1)	98(2)	

[a] Compounds studied: $[\{Cr(CO)_3\}_2\{cyclo\text{-}(C_2H_5AsO)_6\}]$ **1** [8], $[\{ReBr(CO)_2\}_2\{cyclo\text{-}(C_2H_5AsO)_6\}]$ **2**, $[RuCl_2\{cyclo\text{-}(C_2H_5AsO)_6\}(Ph_3P)]$ **3**, $[RhCl_3\{cyclo\text{-}(C_2H_5AsO)_6\}]$ **4**, $[Cu_2\{cyclo\text{-}(C_2H_5AsO)_6\}\text{-}\{(CH_3)_2PhP\}_2](CF_3SO_3)_2$ **5** [45].

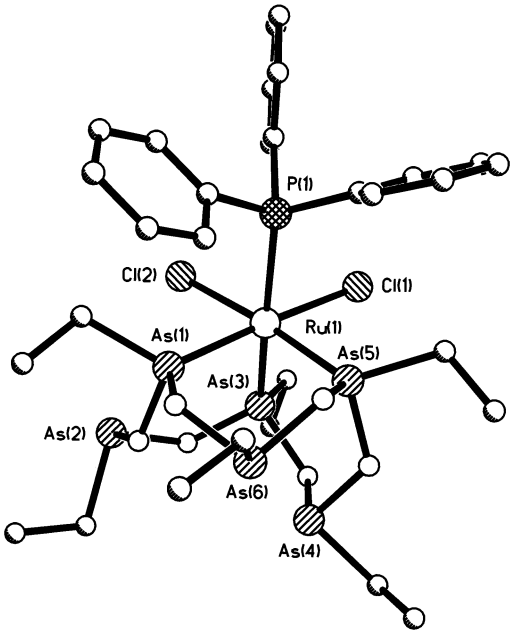

Fig. 16. Molecular structure of $[RuCl_2\{cyclo\text{-}(C_2H_5AsO)_6\}(Ph_3P)]$ (**3**) [45].

either coordinated ($\pm$ 80°) or non-coordinated ($\pm$ 72°). As a result, the latter atoms As2, As4 and As6 (Fig. 17) are now much further apart (average value 3.9 Å) than those in the Rh(III) coordination sphere (average value 3.57 Å). It is apparent that the energetic advantage gained by coordination of a second $RhCl_3$ fragment must

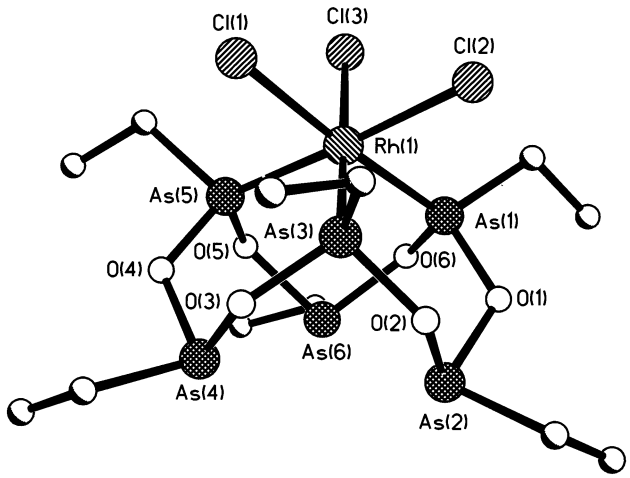

Fig. 17. Molecular structure of $[RhCl_3\{cyclo\text{-}(C_2H_5AsO)_6\}]$ (**4**) [45].

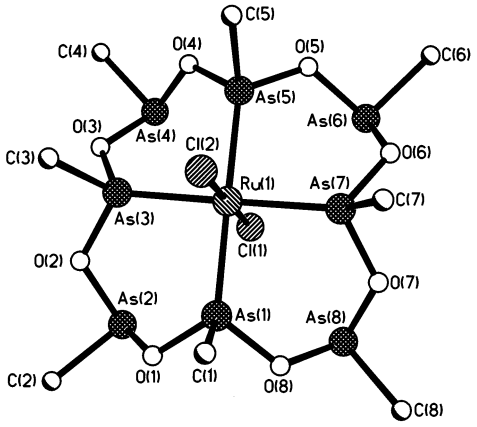

Fig. 18. Molecular structure of $[RuCl_2\{cyclo\text{-}(CH_3AsO)_8\}]$ [46].

be insufficient to compensate for the further increase in ring strain that would be necessary to reduce the former As···As′ distances to ca. 3.57 Å. Interestingly, the markedly larger As–M–As′ angles (103°) required by a Cu(I) tetrahedral coordination sphere lead to longer As···As′ separations (3.73 Å), thereby allowing $(C_2H_5AsO)_6$ to adopt a bridging role in the dicopper complex **5**, despite its relatively short Cu–As distance (2.38 Å).

2.2.3.3. Cyclooctamers $(RAsO)_8$. Reaction of $MCl_3{\cdot}xH_2O$ (M = Ru, Os) with $(CH_3AsO)_n$ at a molar ratio of 1:10 (for $n = 1$) enables the metal-mediated ring expansion of methylcycloarsoxane to an unprecedented cyclooctamer, that is stabilised in the equatorial coordination plane of the resulting octahedral complexes $[MCl_2\{cyclo\text{-}(CH_3AsO)_8\}]$ [46]. The reduction of M(III) to M(II) is accompanied by ligand cleavage and oxidation to $CH_3AsO(OH)_2$. Inspection of the As–Ru–As angles [average values 90(1) and 177.5(2)°] and Ru–As distances [2.400(4) Å] for the Ru(II) complex shown in Fig. 18 confirm the suitability of the very flexible As_8O_8 16-membered ring for its adopted coordination role. As–O distances to the coordinated arsenic atoms As1, As3, As5 and As7 are on average [1.758(8) Å] much shorter than those to the remaining non-coordinated Group 15 atoms [1.799(7) Å]. A concomitant widening of the O–As–O angles for the former atoms is apparent [99.7(4) vs. 97.0(2)°]. The As_8O_8 ring exhibits a double-crown conformation with a torsion angle pattern of the type $(a, b, -b, -a)_4$, where the absolute value of a varies between 104.5 and 124.3° and that for b between 59.5 and 75.0°.

2.3. Coordination polymers

2.3.1. Crystal engineering principles

The rational design of porous solid-state coordination networks capable of hosting guest molecules in their voids has aroused considerable current interest [47–50]. Although the majority of known examples involve tetrahedrally coordi-

nated Ag(I) or Cu(I) atoms separated by rigid organic spacer molecules (e.g. piperazine, pyrazine, 4,4′-bipyridine and 4,4′-biphenyldicarbonitril) a few encouraging reports on the employment of more flexible connecting ligands such as methylene bridged dichalcogenoethers [51] or thioether macrocycles [52–54] have appeared in the recent literature. In analogy to the porous networks of zeolites [55] or Group 14–15 chalcogenidometalates [56,57], these layers or frameworks might be expected to be capable of undergoing elastic deformations in response to different structure-directing agents or imbibed molecular guests.

The successful development of a relatively comprehensive mineralomimetic chemistry based on M–CN–M linkages [58] confirms that the rational design of solid-state coordination polymers is a feasible objective. However extension of these crystal engineering principles to the construction of coordination polymers with larger well-defined cavities is often foiled by the self-interpenetration of multiple networks, which eliminates the void space. This phenomenon is particularly typical for diamondoid networks [49] for which as many as eight or nine interweaving frameworks can be obtained [59–61]. As for organoporous hosts [62], rational crystal engineering principles must enable the systematic modification of solid-state coordination networks and control of cavity size and chemical environment, whilst retaining the supramolecular architecture and preventing lattice interpenetration. A further objective must be the ability of a particular host lattice to accommodate different types of guests by allowing the systematic introduction of molecular building blocks with tailored properties (e.g. non-linear optics, macrocyclic ionophores, chiral functional groups).

Their characteristic ability to bridge tetrahedrally coordinated metal atoms, their pronounced conformative flexibility and their confirmed ion ligating properties suggested to us that cyclotetramers of the type $(RAsO)_4$ might exhibit considerable potential as spacer molecules for the construction of porous coordination lattices with an ability to host a variety of guests (e.g. alkali cations, hydrogen bonding organic molecules). Our previous studies have concentrated on the design of neutral or negatively charged host networks but there is no apparent reason why alkylcycloarsoxanes should not also be employed for the synthesis of positively charged coordination polymers.

We have established three basic design principles for the construction of $(RAsO)_4$ ($R = CH_3$, C_2H_5) bridged networks of copper(I) halides. The self-assembly of a particular supramolecular architecture from $(RAsO)_n$ and CuX (X = Cl, Br, I) is dependent on the molar ratio $(RAsO)_4$:CuX employed, the reaction conditions, the presence of guest molecules to occupy voids, the steric requirements of the alkyl side chains and the propensity of bridging halogen atoms X to extend their coordination number from two to three.

2.3.1.1. $^1_\infty$*[(CuX)$_n${cyclo-(RAsO)$_4$}] ribbons, motif 1.* Two typical examples for such infinite chains are illustrated in a schematic manner in Fig. 19 for (a) a $(CuX)_2$ four-membered ring and (b) a discrete tricyclic $(CuX)_4$ molecular building block. The construction of ribbons as structural motifs has also been observed for a variety of other copper(I) halide moieties, for instance $(CuX)_3$ six-membered rings

and tricyclic Cu_6X_6 units, in which a central four-membered ring is fused to two such flanking $(CuX)_3$ rings. It is apparent that in each case two Cu(I) atoms of the $(CuX)_n$ ($n = 2$, 4) units in the $^1_\infty[(CuX)_n\{cyclo\text{-}(RAsO)_4\}]$ chains of Fig. 19(a,b) exhibit a vacant coordination site and this can be occupied either by terminal monodentate or bridging bidentate ligands. The latter connectivity pattern generates a porous 4^4 net in which the bridging pillars can be either further alkylcycloarsoxanes as in the case of $^2_\infty[(CuX)_2\{cyclo\text{-}(CH_3AsO)_4\}_2]$ (X = Cl, Br, I [40]) or rigid aromatic spacer molecules as illustrated schematically in Fig. 20 for $^2_\infty[Cu_2X_2(p\text{-}H_2NC_6H_4NH_2)\{cyclo\text{-}(CH_3AsO)_4\}]$ [43].

2.3.1.2. $^2_\infty[Cu_3X_3\{cyclo\text{-}(RAsO)_4\}]$ sheets, motif 2. This structural motif is depicted in schematic manner in Fig. 21. Tetradentate twist-chair shaped cyclotetramers $(RAsO)_4$ bridge parallel infinite $^1_\infty[CuX]$ chains to afford a porous sheet in which two thirds of the Cu(I) atoms exhibit a vacant coordination position. Whereas

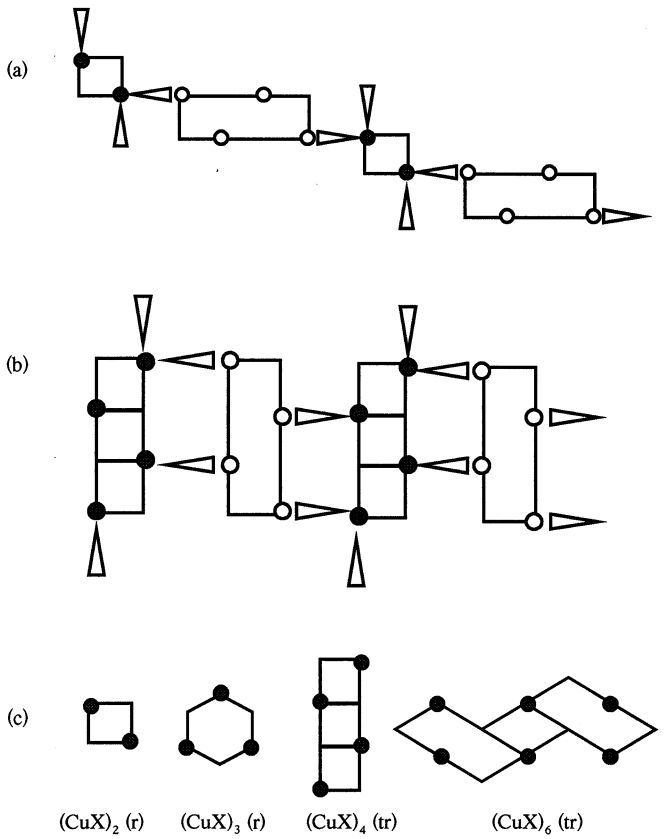

Fig. 19. Schematic representation of two types of $^1_\infty[(CuX)_n\{cyclo\text{-}(RAsO)_4\}]$ ribbon (motif 1): (a) $n = 2$, (b) $n = 4$. Cartoons for various $(CuX)_n$, $n = 2$, 3, 4 and 6 are illustrated in (c). r, ring; c, chain; tr, tricyclic unit.

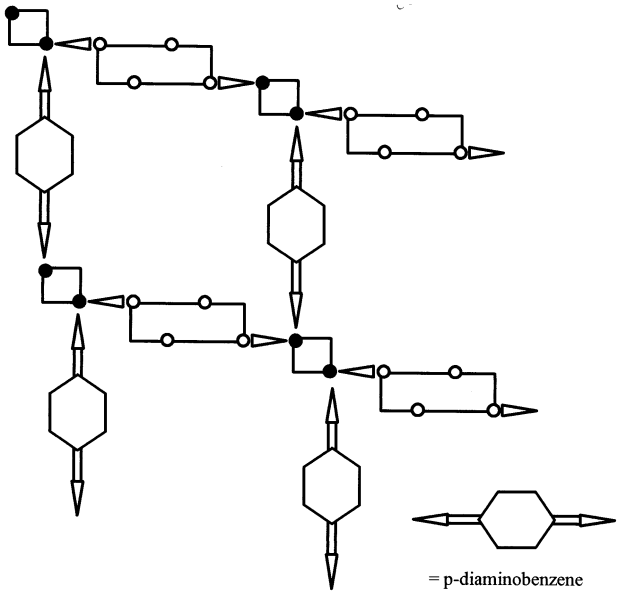

Fig. 20. Schematic representation of the 4^4 planar net of $^{2}_{\infty}[Cu_2I_2(p\text{-}H_2NC_6H_4NH_2)\{cyclo\text{-}(CH_3AsO)_4\}]$ [43].

occupation by a terminal ligand (e.g. CH_3CN) preserves the dimensionality, introduction of a bridging ligand allows the construction of a 3-D framework as in $^{3}_{\infty}[Cu_3X_3\{cyclo\text{-}(CH_3AsO)_4\}_2]$ (X = Cl, Br [40]).

2.3.1.3. $^{2}_{\infty}[Cu_2X_2\{cyclo\text{-}(RAsO)_4\}_3]$ *sheets, motif 3.* This very open network (Fig. 22) has only previously been observed for a copper(I) halide-poor complex with

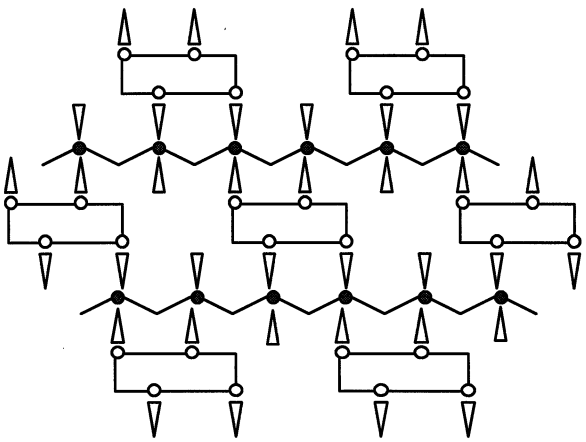

Fig. 21. Schematic representation of the $^{2}_{\infty}[Cu_3X_3\{cyclo\text{-}(RAsO)_4\}]$ sheet, motif 2.

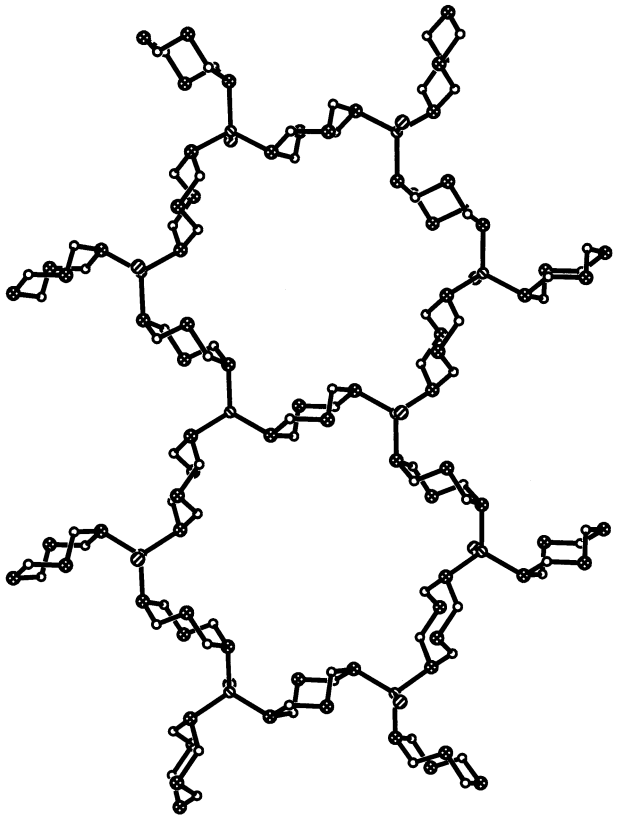

Fig. 22. The 6^3 net $^2_\infty[Cu_2X_2\{cyclo\text{-}(RAsO)_4\}_3]$, motif 3, illustrated for X = Br, R = C_2H_5 [34].

X = Br, R = C_2H_5 [34]. The presence of either bulky side chains R (e.g. R = C_2H_5) or guest template molecules will be necessary to fill the voids provided by the large 36-membered pores. Replacement of terminal halides by bridging pillar ligands to neighbouring sheets could allow the construction of novel open 3-D frameworks.

We will now consider individual examples of CuX coordination polymers formed by the tetraalkylcyclotetraarsoxanes $(CH_3AsO)_4$ and $(C_2H_5AsO)_4$.

2.3.2. Bridging cyclotetramers $(CH_3AsO)_4$

$^2_\infty[Cu_2X_2\{cyclo\text{-}(CH_3AsO)_4\}_2]$ sheets (Cu:X:As ratio = 2:2:8, X = Cl, Br, I) may be obtained by self-organisation of CuX and $(CH_3AsO)_n$ in acetonitrile over a wide range of low Cu:As starting ratios. Fig. 23 displays the layered structure of the isostructural chloride and bromide, in which $^1_\infty[Cu_2X_2\{cyclo\text{-}(CH_3AsO)_4\}]$ ribbons (motif 1) are bridged by bidentate $(CH_3AsO)_4$ pillars to afford a porous 4^4 net with large 28-membered $Cu_6X_2(As_3O_2)_4$ rings of potentially ionophoric character. Translation related sheets exhibit weak secondary X···As interactions of 3.516 (X = Cl) and 3.567 Å (X = Br) and stack so as to generate wide channels, whose cross-sec-

tions are defined by the dimensions of the 28-membered rings. Although the analogous μ-1κAs^1:2κAs^3–$(CH_3AsO)_4$ bridged copper(I) iodide, $^2_\infty[Cu_2I_2\{cyclo\text{-}(CH_3AsO)_4\}_2]$, contains a similar 4^4 net it is not isotypic to the CuCl and CuBr coordination polymers. The 28-membered $Cu_6I_2(As_3O_2)_4$ rings are now elongated in the direction of the transannular Cu···Cu vectors of the $(CuI)_2$ building unit, i.e. effectively at right angles to the distortion observed for X = Cl, Br (Fig. 23). Once again, individual layers are connected through very weak interactions (I···As 4.101 Å), providing wide tunnels of pore size 4.1×7.2 Å as gauged by the shortest transannular H···H contacts.

When the self assembly reaction between CuI and $(CH_3AsO)_n$ is performed in C_6H_5CN instead of CH_3CN, the connectivity role of the $(CH_3AsO)_4$ pillars is taken over by terminally κN coordinated solvent molecules, whose aromatic π-systems stack to construct a 3-D network, the component layers of which are displayed in Fig. 24 [43]. The voids generated by these stacking interactions are spacious enough (8.2×8.2 Å) to accommodate relatively large guest C_6H_5CN molecules. We have extended this design principle (Fig. 20) to the bridging aromatic spacer molecules p-$NH_2C_6H_4NH_2$ [43] and p-$NH_2C_{12}H_8NH_2$ [63]. Deep-red crystals of the layered structure $^2_\infty[Cu_2I_2\ (p\text{-}H_2NC_6H_4NH_2)\{cyclo\text{-}(CH_3AsO)_4\}]$ may be grown by carefully underlayering a p-$H_2NC_6H_4NH_2/(CH_3AsO)_n$ solution in CH_3CN with a CuI solution in the same solvent at 0°C. The ordered alignment of the aromatic chromophores in this 4^4 net (Fig. 25) implies that its absorption of electromagnetic

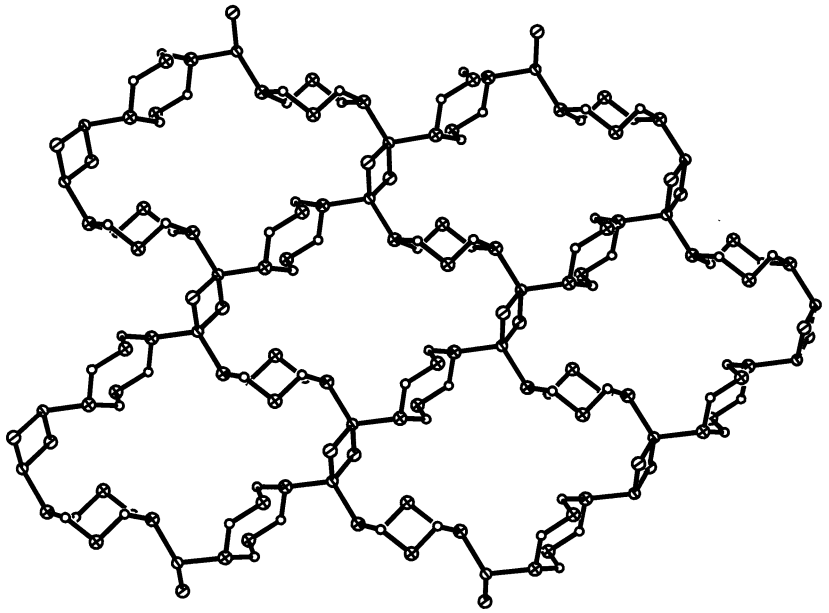

Fig. 23. Structure of $^2_\infty[Cu_2X_2\{cyclo\text{-}(CH_3AsO)_4\}_2]$ (X = Cl, Br, [40]) in which $^1_\infty[Cu_2X_2\{cyclo\text{-}(CH_3AsO)_4\}]$ ribbons (motif 1) are linked by $(CH_3AsO)_4$ pillars into a porous 4^4 net. Methyl groups have been omitted for clarity.

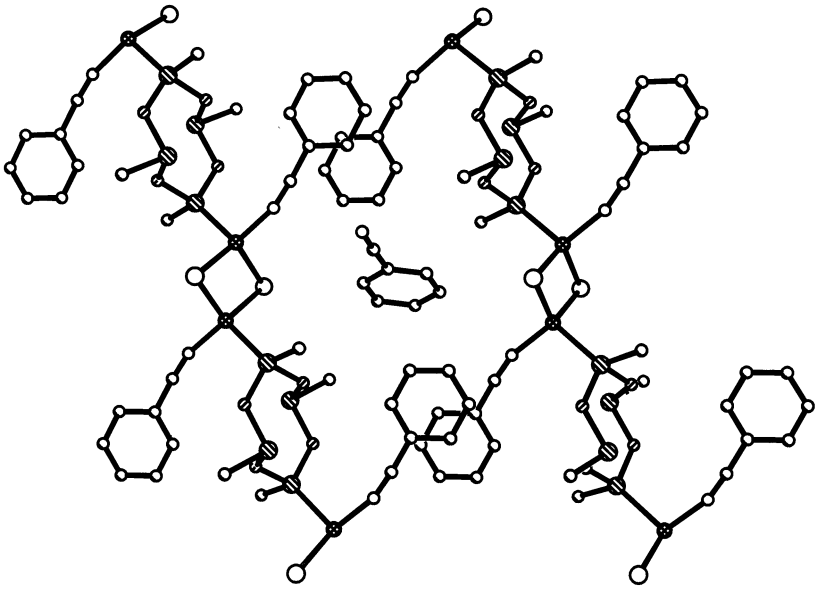

Fig. 24. Packing diagram for the $\pi-\pi$ stacked chains of $^{1}_{\infty}[Cu_2I_2(C_6H_5CN)_2\{cyclo\text{-}(CH_3AsO)_4\}]$. The resulting wide channels accommodate guest C_6H_5CN solvent molecules [43].

radiation must be anisotropic. Optical properties of zeolites with analogous imbibed parallel chromophore molecules such as *p*-nitroaniline are of considerable technological interest [64]. When $p\text{-}H_2NC_{12}H_8NH_2$ pillars are employed instead of $p\text{-}H_2NC_6H_4NH_2$, the larger cavities accommodate disordered acetonitrile solvent molecules [65].

The ribbon motif 1 (Fig. 19a) has also been found in the CuX-richer coordination polymers $^{1}_{\infty}[Cu_6Br_6(C_6H_5CN)_4\{cyclo\text{-}(CH_3AsO)_4\}]$ [32] and $^{2}_{\infty}[Cu_4I_4\{cyclo\text{-}(CH_3AsO)_4\}_2]$ [41]. Tricyclic Cu_6Br_6 building blocks are linked in the former complex into a 1-D polymer by bridging κ^4As coordinated cyclotetramers $(CH_3AsO)_4$, which once again adopt the characteristic twist-chair conformation (tc4 mode). As may be seen in Fig. 26, symmetry-related C_6H_5CN molecules on opposite sides of the infinite chains are orientated away from the propagation vector of the coordination polymer and this allows their aromatic π-systems to stack with those of the analogous terminal solvent molecules from neighbouring chains to afford a network similar to that of $^{1}_{\infty}[Cu_2I_2(C_6H_5CN)_2\{cyclo\text{-}(CH_3AsO)_4\}]$ (Fig. 24).

$^{2}_{\infty}[Cu_4I_4\{cyclo\text{-}(CH_3AsO)_4\}_2]$ may be obtained by self-assembly from CuI and $(CH_3AsO)_n$ in acetonitrile at Cu:As starting ratios between 0.375 and 2.0. Whereas lower Cu:As ratios afford the previously described lamellar compound $^{2}_{\infty}[Cu_2I_2\{cyclo\text{-}(CH_3AsO)_4\}_2]$, higher Cu:As ratios lead to sole formation of $^{2}_{\infty}[\{CuI(CuI{\cdot}CH_3CN)_2\}\{cyclo\text{-}(CH_3AsO)_4\}]$ with motif 2, which will be discussed subsequently. A total of 75% of the potential As coordination sites are employed in $^{2}_{\infty}[Cu_4I_4\{cyclo\text{-}(CH_3AsO)_4\}_2]$ whose sheet structure is displayed in Fig. 27. All four

As atoms of one of the independent $(CH_3AsO)_4$ ligands participate in copper binding to atoms of tricyclic Cu_4I_4 building blocks, thereby providing $^1_\infty[Cu_4I_4\{cyclo\text{-}(CH_3AsO)_4\}]$ ribbons (motif 1) running in direction [010]. μ-$1\kappa As^1{:}2\kappa As^3$ coordinated $(CH_3AsO)_4$ pillars link adjacent chains to construct a porous sheet with large $[Cu(As_2O)(Cu_2I)(As_2O)]_2$ rings.

A higher CuX:As ratio of 0.75 is achieved in the isotypic lamellar polymers $^2_\infty[\{CuX(CuX{\cdot}CH_3CN)_2\}\{cyclo\text{-}(CH_3AsO)_4\}]$ (X = Br, I) [41] by incorporation of acetonitrile solvent molecules at the vacant coordination sites of two thirds of the Cu(I) atoms of an infinite $^1_\infty[CuX]$ single chain (structural motif 2, Fig. 21). As depicted in Fig. 12 for X = Br, adjacent copper(I) halide chains are linked through crystallographically centrosymmetric $\kappa^4 As$ coordinated $(CH_3AsO)_4$ ligands into the

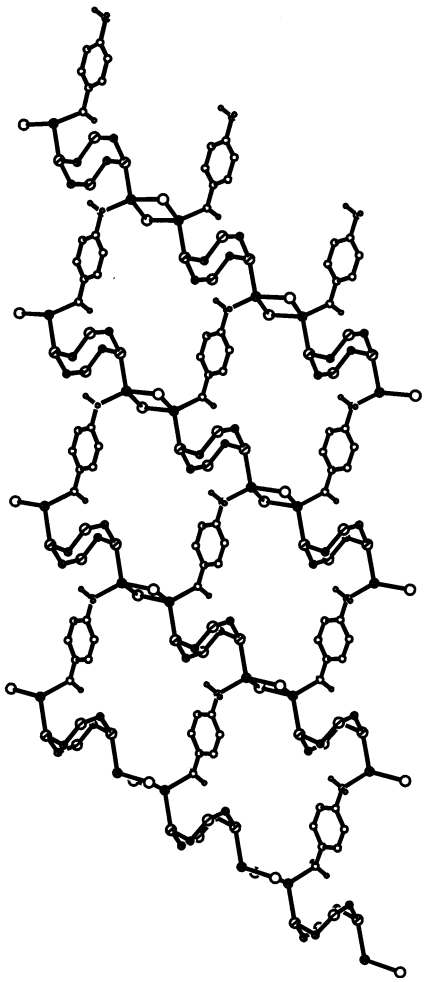

Fig. 25. Structure of the lamellar $^2_\infty[Cu_2I_2(p\text{-}H_2NC_6H_4NH_2)\{cyclo\text{-}(CH_3AsO)_4\}]$ 4^4 net [43]. Methyl groups have been omitted for clarity.

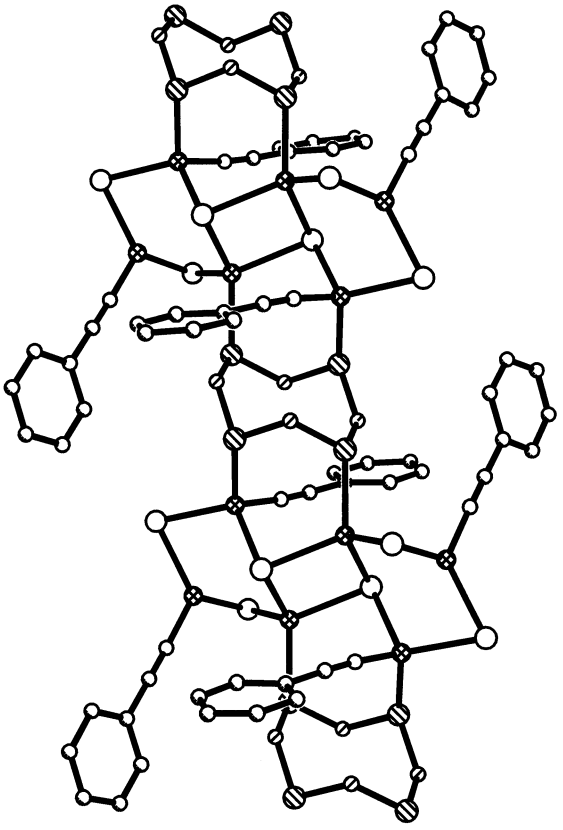

Fig. 26. Chain structure of $^{1}_{\infty}[Cu_6Br_6(C_6H_5CN)_4\{cyclo\text{-}(CH_3AsO)_4\}]$ [32]. Methyl groups have been omitted for clarity.

porous sheet structure with 16-membered $[Cu_3X_2(As_2O)]_2$ rings presented in Fig. 28. Whereas Cu(1) and Br(1) in Fig. 12 both lie on crystallographic twofold rotation axes of the monoclinic space group $C2/c$, the remaining atoms of the polymeric $^{1}_{\infty}$[CuBr] single chains, Cu(2) and Br(2), occupy general positions. A remarkable difference is apparent for the independent Cu–X–Cu chain angles in these isotypic compounds, where Cu(1)–X(1)–Cu(2) angles of 94.8(1) (X = Br) and 90.8(1)° (X = I) within the six-membered $[Cu_2X(As_2O)]$ rings contrast with wide Cu(2)–X(1)–Cu(2)′ angles of 148.2(1) (X = Br) and 143.1(1)° (X = I).

The $^{2}_{\infty}[Cu_3X_3\{cyclo\text{-}(CH_3AsO)_4\}]$ sheets of structural motif 2 (Fig. 21) can also be identified in the unique open 3-D networks of the isotypic compounds $^{3}_{\infty}[Cu_3X_3\{cyclo\text{-}(CH_3AsO)_4\}_2]$ (X = Cl, Br) [40]. Opposite arsenic atoms of μ-$1\kappa As^1{:}2\kappa As^3$ bridging $(CH_3AsO)_4$ ligands now occupy the vacant coordination sites of two thirds of the Cu(I) atoms of the $^{1}_{\infty}$[CuX] ribbons and connect neighbouring sheets to generate the porous framework structure depicted in Fig. 29. The presence of both non-coordinated and coordinated arsenic atoms in $^{3}_{\infty}[Cu_3X_3\{cyclo\text{-}$

$(CH_3AsO)_4\}_2]$ (X = Cl, Br) leads to the pronounced splitting of the ν(As–O) IR absorption bands in the range 720–760 cm^{-1}. Whereas the position of the ν(As–O) at respectively 733 (X = Cl) and 730 cm^{-1} (X = Br) remains effectively unchanged for the non-coordinated As atoms in comparison to $(CH_3AsO)_4$ itself (724 cm^{-1}), strengthening of the As–O bonds to the coordinated arsenic atoms causes a shift in this absorption band to higher wavenumbers for X = Cl (749 cm^{-1}) and X = Br (758 cm^{-1}) [40]. Analogous shifts of ca. 20–35 cm^{-1} were observed in other methylcycloarsoxane complexes.

As reviewed in Section 2.2.2, alkylcycloarsoxanes coordinate alkali metal cations M in a $\kappa^n O$ fashion in sandwich complexes of the type $[M\{cyclo\text{-}(RAsO)_n\}_2]$ (M = Na; $n = 4$; M = K, Cs; $n = 5$). The presence of immobilised cyclic ionophores in the coordination polymers previously described in this Section suggested to us that the self-assembly of negatively charged host networks from CuX and $(CH_3AsO)_n$ in solutions containing alkali metal cations should be possible. This goal was then first achieved in the layered structure of $[Cs(H_2O)_2][Cu_3I_4\{cyclo\text{-}(CH_3AsO)_4\}_2]$ depicted in Figs. 30 and 31. Two water ligands were found to be

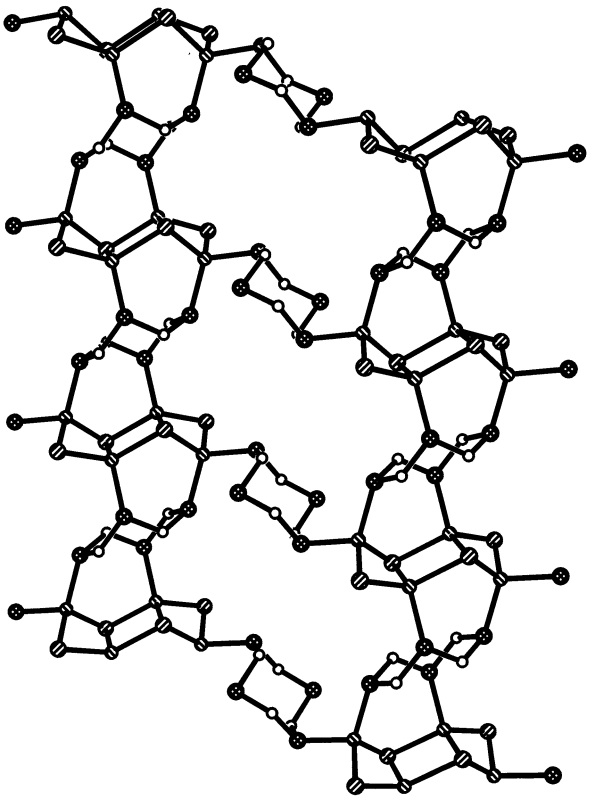

Fig. 27. Layered structure of $^2_\infty[Cu_4I_4\{cyclo\text{-}(CH_3AsO)_4\}_2]$ [41] with methyl groups omitted for the sake of clarity.

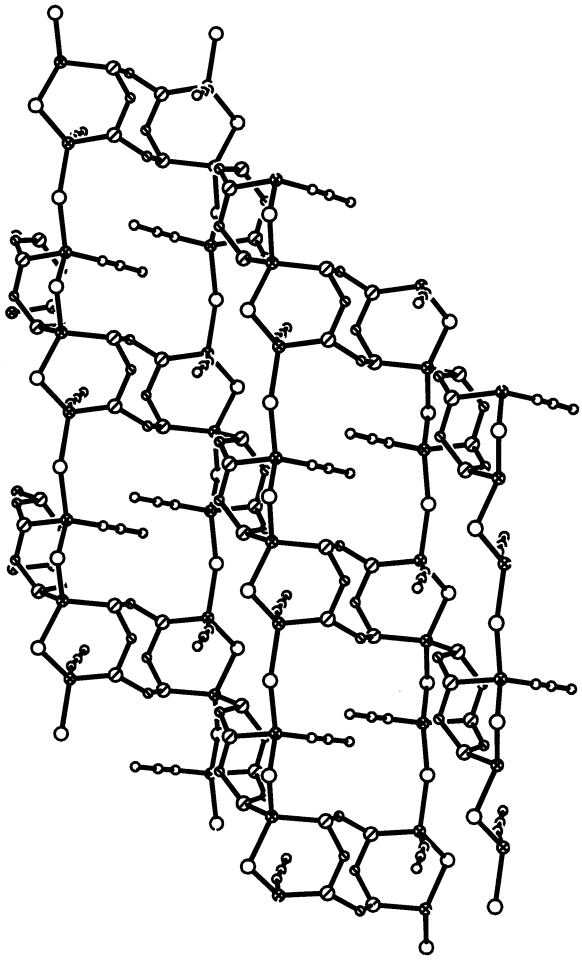

Fig. 28. The sheet structure of $^{2}_{\infty}[\{CuBr(CuBr{\cdot}CH_3CN)_2\}\{cyclo\text{-}(CH_3AsO)_4\}]$ [41] with methyl groups omitted for the sake of clarity.

necessary to complete the tenfold $\kappa^{10}O$ coordination spheres of the Cs^+ cations, used to direct the self-organisation of the anionic $^{1}_{\infty}[Cu_3I_4\{cyclo\text{-}(CH_3AsO)_4\}_2]$ chains from CuI and $(CH_3AsO)_n$ in a $CH_3CN/CH_3OH/H_2O$ mixture [43]. Though preferred for the construction of the 1-D CuI coordination polymers in this structure, the cyclotetramers $(CH_3AsO)_4$ are clearly less well-suited for the coordination of the large Cs^+ cations than would have been cyclopentamers $(CH_3AsO)_5$, as for example the analogous $(C_2H_5AsO)_5$ ligands in $^{1}_{\infty}[\{Cs[cyclo\text{-}(C_2H_5AsO)_5]_2\}Cu_2(\mu\text{-}I)I_2]$ (Fig. 9) [34]. The less favourable open sandwich structure of the $[Cs^+\{cyclo\text{-}(CH_3AsO)_4\}_2]^+$ units and the flexible nature of the anionic ribbons suggest that exchange of the Cs cations by smaller alkali metal cations (Na^+, K^+) could be possible and work is in progress in this direction. Disordered

methanol molecules are located in the relatively large cavities of $[Cs(H_2O)_2][Cu_3I_4\{cyclo\text{-}(CH_3AsO)_4\}_2]$, which exhibit an increased degree of polar character as a result of the presence of H_2O molecules in the cesium coordination sphere. A DTA trace reveals initial endothermic loss of methanol and water (35–120°C) followed by endothermic collapse of the solid-state network in a temperature range (122–149°C) similar to that recorded for other alkylcycloarsoxane-bridged Cu(I) halides. These results indicate that this flexible sheet structure could be capable of imbibing a range of smaller polar molecules whilst retaining its integrity.

A second example of an anionic host network is provided by $^{3}_{\infty}[\{Cs[cyclo\text{-}(CH_3AsO)_4]Cu_3I_4\}\{cyclo\text{-}(CH_3AsO)_4\}]$ [32], in which Cu_3I_3 units are bridged by $(CH_3AsO)_4$ in a μ-1κAs^1:2κAs^3 manner (Fig. 14) into $^{1}_{\infty}[Cu_3I_3\{cyclo\text{-}(CH_3AsO)_4\}]$ ribbons (motif 1, which themselves are linked by iodine atoms into lamellar anions (Fig. 32). As previously discussed (Section 2.2.3), a second independent cyclote-

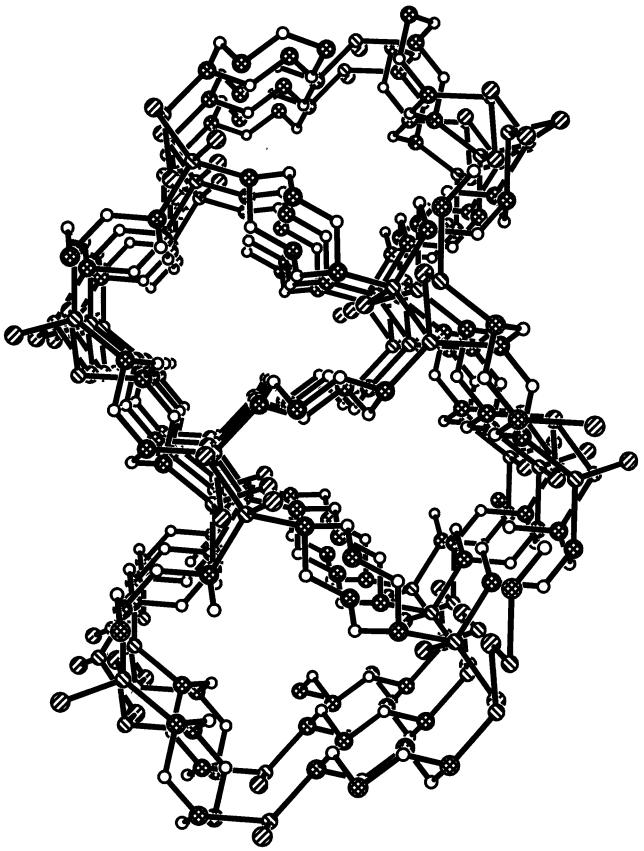

Fig. 29. The porous framework structure of $^{3}_{\infty}[Cu_3Br_3\{cyclo\text{-}(CH_3AsO)_4\}_2]$ [40]. Methyl groups have been omitted for clarity.

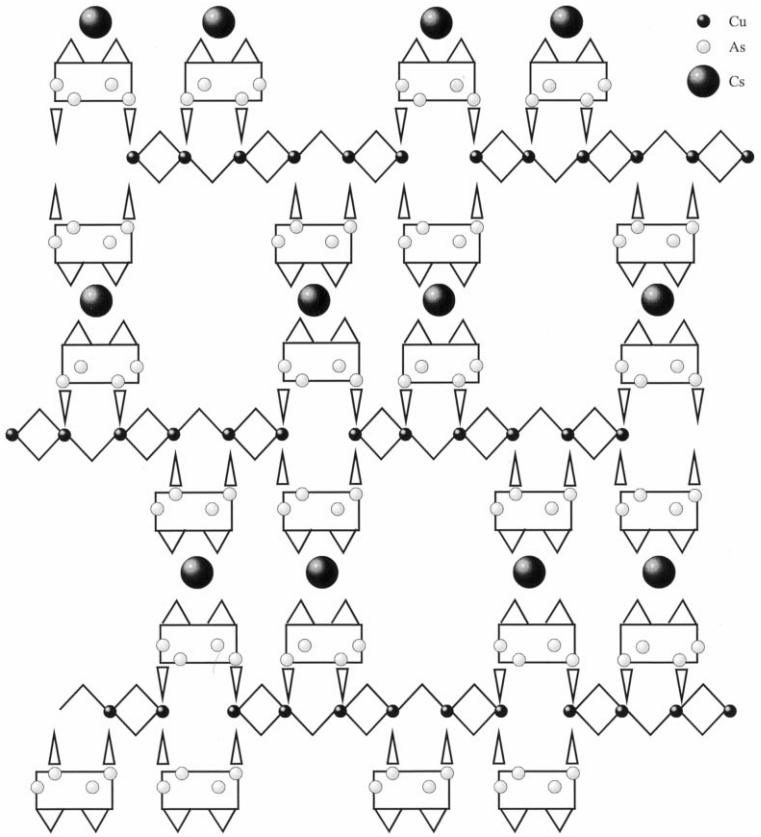

Fig. 30. A schematic diagram of the building principle of the layered structure of $[Cs(H_2O)_2][Cu_3I_4\{cyclo\text{-}(CH_3AsO)_4\}_2]$ [43].

tramer $(CH_3AsO)_4$ adopts a crown conformation and coordinates not only all three Cu(I) atoms of a horseshoe-like Cu_3I_3 building block but also one of the Cs^+ countercations (Fig. 14), responsible for the construction of a 3-D framework.

Despite their striking diversity, all of $(CH_3AsO)_4$ bridged polymeric CuX networks listed in Table 3 can, with one exception, be assigned to either structural motif 1 or 2. The exception, $^1_\infty[\{(CuBr)_2(CuBr{\cdot}CH_3CN)_2\}\{cyclo\text{-}(CH_3AsO)_4\}]$ [41], represent an intermediate product on the reaction pathway to $^2_\infty[\{CuBr(CuBr{\cdot}CH_3CN)_2\}\{cyclo\text{-}(CH_3AsO)_4\}]$ (Fig. 21) and may be prepared in acetonitrile solution at a similar $CuBr:(CH_3AsO)_n$ molar ratio by increasing the initial rate of heating between 20°C and the highest reaction temperature 100°C from 2 to 5°C h^{-1}. Its chain structure is illustrated in Fig. 33 and offers an instructive insight into the self-assembly mechanisms involved in the formation of such coordination polymers. The infinite ribbons formed on initial breakdown of the CuBr structure are composed of fused chair-shaped six-membered Cu_3Br_3 rings, in which individual Cu(I) atoms are coordinated by As atoms of crown-shaped

Table 3
Copper(I) halide coordination polymers with bridging $(RAsO)_4$ cyclotetramers

Molar ratio Cu:X:As	Halide X	Motif	Dimension	CuX unit	CuX type	Terminal ligands	Pillar ligands	References
$R = CH_3$								
2:2:8	Cl, Br, I	1	2	$(CuX)_2$	Ring		$(CH_3AsO)_4$	[40]
3:3:8	Cl, Br	2	3	[CuX]	Chain		$(CH_3AsO)_4$	[40]
3:4:8	I	1	1	Cu_6X_8	Chain	$(CH_3AsO)_4$		[43]
2:2:4	I	1	1	$(CuX)_2$	Ring	C_6H_5CN		[43]
2:2:4	I	1	2	$(CuX)_2$	Ring		p-$NH_2C_6H_4NH_2$	[43]
2:2:4	I	1	2	$(CuX)_2$	Ring		p-$NH_2C_{12}H_8NH_2$	[63]
4:4:8	I	1	2	$(CuX)_4$	Tricyclic		$(CH_3AsO)_4$	[41]
3:3:4	Br, I	2	2	$^1_\infty$[CuX]	Chain	CH_3CN		[41]
3:4:4	I	1	2	$(CuX)_3$	Chain	$(CH_3AsO)_4$	I	[32]
4:4:4	Br		1	$^1_\infty[(CuX)_2]$	Double chain	CH_3CN		[41]
6:6:4	Br	1	1	Cu_6X_6	Tricyclic	C_6H_5CN		[32]
$R = C_2H_5$								
2:2:12	Br	3	2	CuX	Monomer			[34]
4:4:12	Cl	1	1	$(CuX)_3CuX$	Ring	$(C_2H_5AsO)_4$		[42]
3:3:8	Br, I	1	2	$(CuX)_2$	Ring	$(C_2H_5AsO)_4$	$(XCu)_2$	[34,42]
6:6:12	I		2	$(CuX)_2Cu$	Ring	$(C_2H_5AsO)_4$	I	[42]

$(CH_3AsO)_4$ ligands. Whereas two of the crystallographically independent bromine atoms exhibit their maximal coordination of 3, the remaining two such atoms are each involved in only two Cu–Br interactions. The resulting free fourth coordination positions on two copper atoms are occupied by solvent acetonitrile molecules. Cleavage of the shared Cu–Br bonds of the fused Cu_3Br_3 rings to afford parallel $(CH_3AsO)_4$ bridged infinite $^1_\infty$[CuBr] ribbons and subsequent condensation of these polymeric units to layers leads to construction of $^2_\infty$[{CuBr(CuBr·$CH_3CN)_2$}{*cyclo*-$(CH_3AsO)_4$}] (motif 2) with only a limited degree of associated structural reorganisation. An alternative initial cleavage of opposite Cu–Br bonds within the individual CuBr ribbons of the original $^1_\infty[Cu_2Br_2]$ double chains would generate the $(CH_3AsO)_4$ linked discrete $(CuBr)_n$ units, found in the infinite $^1_\infty$[$(CuBr)_n${*cyclo*-$(CH_3AsO)_4$}] chains of motif 1.

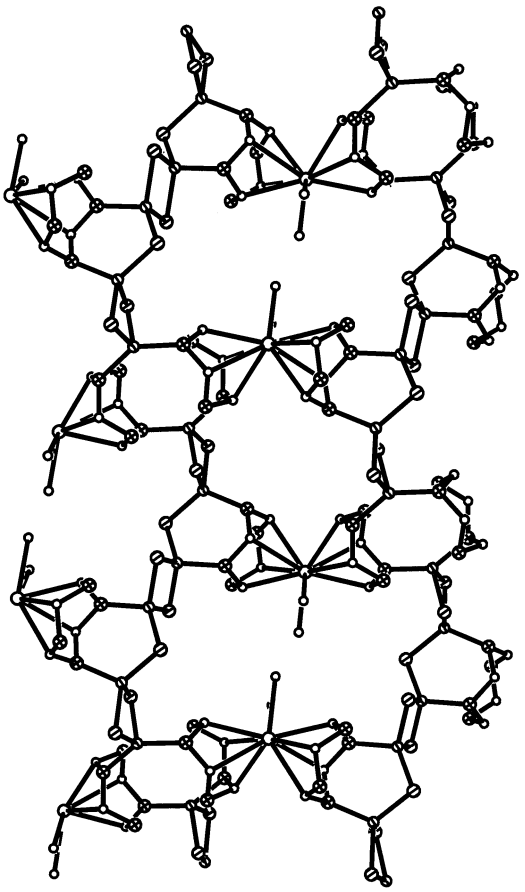

Fig. 31. Packing diagram for the anionic chains that are linked through $[Cs\{cyclo\text{-}(CH_3AsO)_4\}_2]^+$ sandwiches into a porous sheet in $[Cs(H_2O)_2][Cu_3I_4\{cyclo\text{-}(CH_3AsO)_4\}_2]$ [43]. Methyl groups have been omitted for clarity.

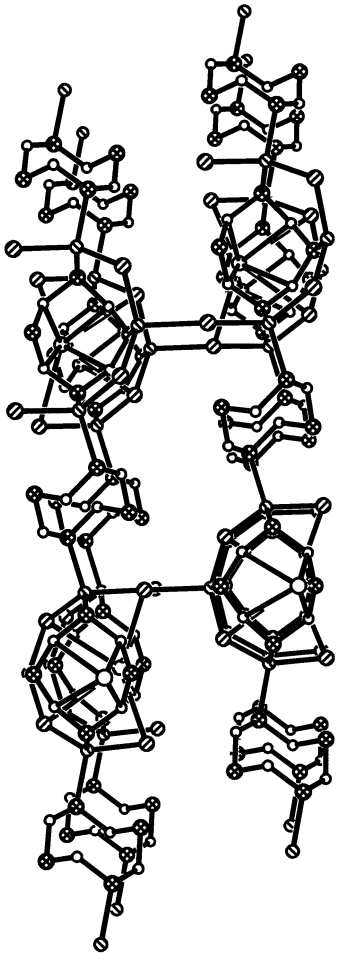

Fig. 32. The framework structure of $^{3}_{\infty}$[{Cs[*cyclo*-$(CH_3AsO)_4$]Cu_3I_4}{*cyclo*-$(CH_3AsO)_4$}] [32] with methyl groups omitted for the sake of clarity.

2.3.3. Bridging cyclotetramers $(C_2H_5AsO)_4$

The steric requirements of the hydrophobic alkyl side chains will be expected to influence the construction of $(RAsO)_4$ bridged copper(I) halides networks. It is, therefore, of interest to compare the solid-state structures for the more voluminous ethyl groups with those adapted for $R = CH_3$. Inspection of Table 3 indicates that far fewer coordination polymers have been characterised for the former alkyl side chain and that those that are known are all relatively CuX-poor (CuX:As ≤ 0.5).

The bulkiness of the ethyl groups allows the construction of the unique 6^3 nets (Fig. 22) in $^{2}_{\infty}$[Cu_2Br_2{*cyclo*-$(C_2H_5AsO)_4$}$_3$] (structural motif 3) [34] in contrast to the characteristic 4^4 nets found in the CuX-poor complexes of the type $^{2}_{\infty}$[Cu_2X_2{*cyclo*-$(CH_3AsO)_4$}$_2$] (X = Cl, Br, I) (see Fig. 23) [40]. The associated

expansion of the pore size from 28 to 36 ring members on going from $R = CH_3$ to $R = C_2H_5$ reflects the increased steric requirements of the larger alkyl side chains, which fill the voids created by the CuX bridged arsoxane network.

Typical for $(C_2H_5AsO)_4$ coordination polymers of copper(I) halides with a CuX:As molar ratio of 0.333–0.50 is the presence of cage-like $[Cu_3X(As_4O_4)]$ building blocks, in which three of the arsenic atoms of a crown-shaped $(AsO)_4$ ring are bridged by a $[Cu_3(\mu_3\text{-}X)]$ unit. The asymmetric unit of $^1_\infty[Cu_4Cl_4\{cyclo\text{-}(C_2H_5AsO)_4\}_3]$ [42] with its independent crown, boat-chair and twist-chair shaped $(C_2H_5AsO)_4$ ligands (Fig. 13) was already discussed in Section 2.2.3.1. The latter heterocycles link the $[Cu_3Cl(As_4O_4)]$ cages into the infinite chains depicted in Fig. 34 (motif 1). A similar structural motif is also present in $^2_\infty[Cu_3X_3\{cyclo\text{-}(C_2H_5AsO)_4\}_2]$ (X = Br, I) [34,42], as may be seen for X = Br in Fig. 35. However, in this case, copper(I) atoms from adjacent ribbons also participate in the shared

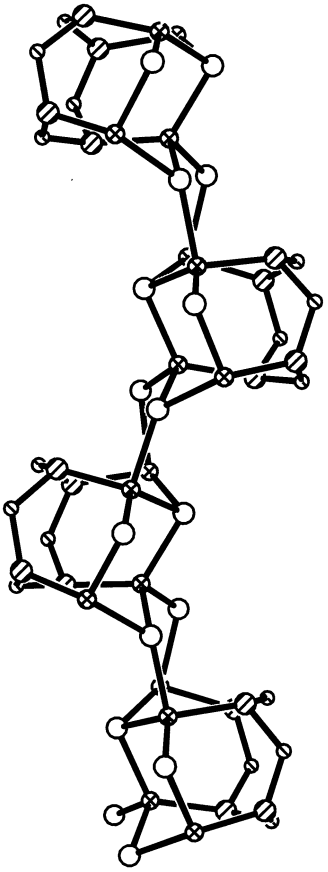

Fig. 33. The infinite chain of $^1_\infty[\{(CuBr)_2(CuBr{\cdot}CH_3CN)_2\}\{cyclo\text{-}(CH_3AsO)_4\}]$ with its $[(Cu_4Br_4)\{cyclo\text{-}(CH_3AsO)_4\}]$ cages [41]. Methyl groups and coordinated acetonitrile molecules have been omitted for clarity.

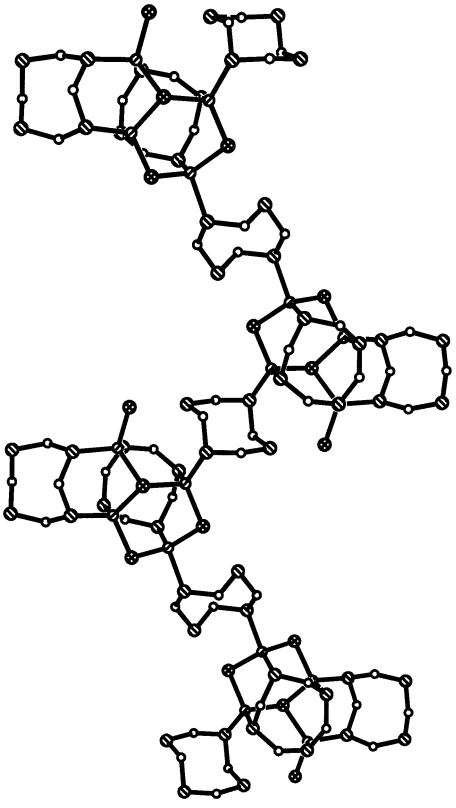

Fig. 34. The polymer chain structure of $^{1}_{\infty}[Cu_4Cl_4\{cyclo\text{-}(C_2H_5AsO)_4\}_3]$ [42] in which ethyl groups have been omitted for the sake of clarity.

$(CuX)_2$ rings, that function as pillars in a porous 2-D network. $[Cu_3I(As_4O_4)]$ cages are also present in the CuX-richer complex $^{2}_{\infty}[Cu_6I_6\{cyclo\text{-}(C_2H_5AsO)_4\}_3]$ [42], which once again exhibits an open lamellar structure. A central $(C_2H_5AsO)_4$ ligand joins two such cages in the tc4 coordination mode to generate large $[Cu_6I_6\{cyclo\text{-}(C_2H_5AsO)_4\}_3]$ building blocks, which corner-bridge through common iodine atoms into the 4^4 net illustrated in Fig. 36. The characteristic presence of relatively large oligonuclear units in the solid-state structures discussed in this Section clearly results from a screening effect of the bulky ethyl side chains.

2.4. Cleavage products of $(RAsO)_n$

We have studied the reaction of K_2PtCl_4, $AgNO_3$ or Ag_2CO_3 and $(CH_3AsO)_n$ at molar ratios between 1:3:6 and 2:3:6 in acetonitrile at 100°C during unsuccessful attempts to stabilise the cyclooctamer $(CH_3AsO)_8$ (see Section 2.2.3.2) in the square-planar coordination sphere of Pt(II). However, two dimeric Pt(II) complexes could be isolated as red crystals in relatively low yields (13–15%) under such

conditions independent of which of the silver salts was employed [46]. To our surprise both contained novel tetradentate bridging ligands, that each result from a metal-mediated reaction between $(CH_3AsO)_n$ and acetonitrile. The structures of these products, $[Pt_2\{cyclo\text{-}[As(CH_3)OAs\{NC(O)CH_3\}O]_2\}_2]$ and $[Pt_2\{[CH_3C(O)N]_2\text{-}As_5(CH_3)_5O_4\}_2]$ are depicted together with their respectively cyclic and acyclic anionic ligands in Figs. 37 and 38. Their Pt–As [2.387(4), 2.382(2) Å] and Pt–N distances [2.04(2), 2.03(2) Å] are very similar and both complexes contain formally trivalent arsenic atoms (As(1), As(3), As(5) and As(7) in Fig. 37, As(2) and As(4) in Fig. 38) with a trigonal bipyramidal coordination geometry, thereby providing, to our knowledge, the first examples of such an environment for As(III). These unique coordination polyhedra are completed by weak axial O···As interactions between bridging ligands, e.g. O(32)···As(5) and O(24)···As(7) in the first complex [average distance 2.20(1) Å] and O(12)···As(4a) and O(22)···As(2a) in the second product [average distance 2.27(1) Å]. The opposite axial O–As bonds in the severely distorted trigonal bipyramids are, as expected, much shorter [1.83(1) and 1.82 (1) Å, respectively].

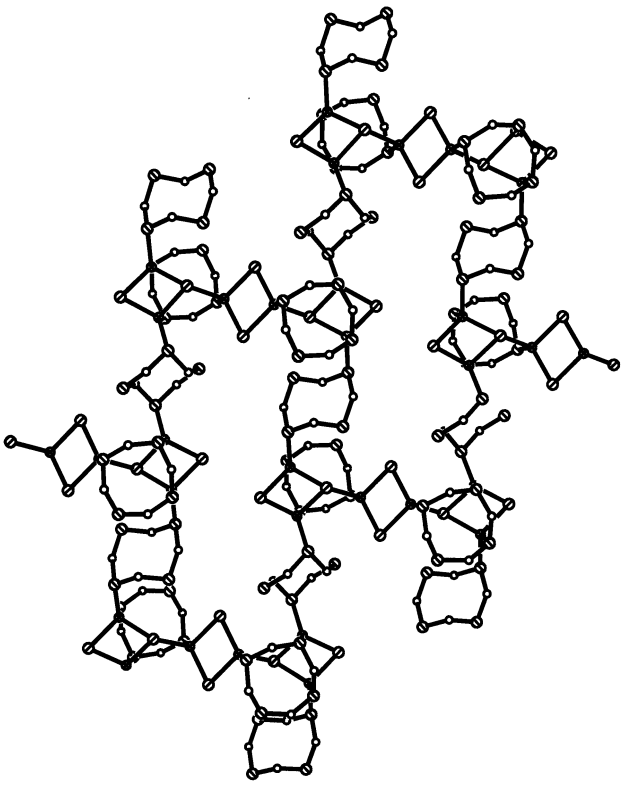

Fig. 35. The porous layer of $^2_\infty[Cu_3Br_3\{cyclo\text{-}(C_2H_5AsO)_4\}_2]$ [42] in which $(CuBr)_2$ pillar units connect ribbons of structural motif 1. Ethyl groups have once again been omitted.

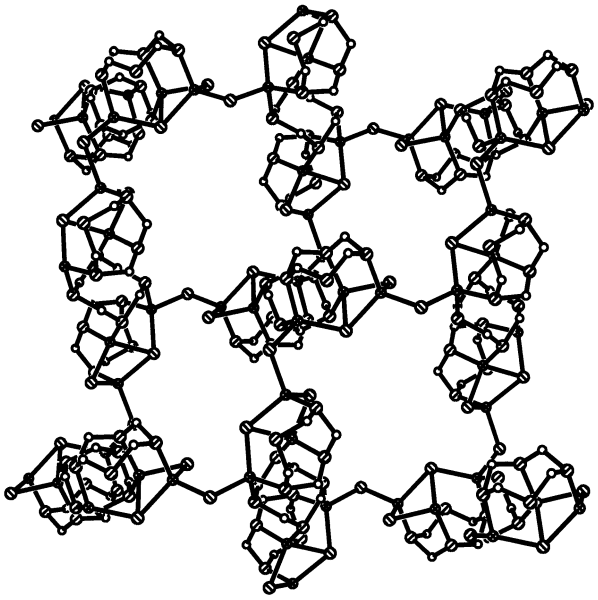

Fig. 36. The open 4^4 net of $^{2}_{\infty}[Cu_6I_6\{cyclo\text{-}(C_2H_5AsO)_4\}_3]$ [42] with corner-bridged $[Cu_6I_6\{cyclo\text{-}(C_2H_5AsO)_4\}_3]$ building blocks.

As hydrolysis of alkylcycloarsoxanes is facile, solvents for these cyclic ligands must be carefully dried before use. Indeed, even the presence of water molecules of crystallisation in a starting compound can be adequate to promote the cleavage of As–C bonds. For instance, $[RhCl_3\{As_5(C_2H_5)_2O_5(OH)_2\}]$ (Fig. 39) is obtained as a minor product of the reaction between $RhCl_3{\cdot}3H_2O$ and $(C_2H_5AsO)_n$ in acetone [66]. Interestingly this compound contains a six-memebered $(AsO)_3$ ring, i.e. of a size not found in complexes of the parent cycloarsoxane.

3. Coordination chemistry of organylcycloarsathianes

3.1. Preparation and structure of $(RAsS)_n$

As summarised by Tzschach and Heinicke in their book on heterocyclic arsenic compounds [20], organylcycloarsathianes $(RAsS)_n$ are generally obtained by either (a) treatment of $RAsX_2$ (X = Cl, Br) with H_2S or sulphides [15], (b) oxidation of primary arsines with sulphur [67] or (c) reaction of arsines with $SOCl_2$ [68] or PhNSO [16]. Organylcycloarsoxanes $(RAsO)_n$ can be converted to their sulphur analogues by treatment with H_2S [3,12].

Molecular weight and ^{1}H-NMR studies indicate that cyclotrimers $(RAsS)_3$ and cyclotetramers $(RAsS)_4$ clearly predominate in organic solutions of alkylcycloarsathianes [12,15–17]. DiMaio and Rheingold [18] were successful in separating

these cyclic oligomers for $R = CH_3$ both in solution by column chromatography with alumina and in the solid state by microscopic selection of crystals on the basis of their different morphologies. The respectively chair and crown conformations of the alternating As–S rings in $(CH_3AsS)_3$ and $(CH_3AsS)_4$ are depicted in Fig. 40. Whereas the average As–S distances [2.258 (1), 2.249 (5) Å] and S–As–S angles [101.4 (2), 102.5 (7)°] are similar in both cyclic oligomers, a marked widening of the average As–S–As angle from 93.8 (2) to 98.2 (7)° is apparent on going from the chair to the crown conformation. The latter structure has also been established for the tetramers $(C_2H_5AsS)_4$ [12], $(t\text{-}C_4H_9AsS)_4$ [13] and $(PhAsS)_4$ [14] in the solid state.

3.2. Coordination properties of $(C_2H_5AsS)_4$

Both S and As are potential soft donor atoms for transition and coinage metals M in their lower oxidation states. Employing average metrical parameters from the solid state structures of $(CH_3AsS)_4$ and $(C_2H_5AsS)_4$, Fig. 41 illustrates the dependence of As–M–As and S–M–S angles in hypothetical four-membered chelate

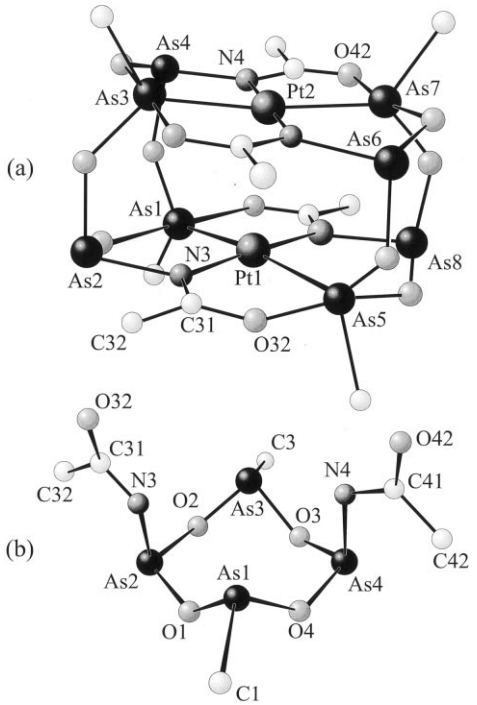

Fig. 37. (a) Molecular structure of $[Pt_2\{cyclo\text{-}[As(CH_3)OAs\{NC(O)CH_3\}O]_2\}_2]$ prepared by reaction of K_2PtCl_4, $AgNO_3$ and $(CH_3AsO)_n$ in acetonitrile at 100°C. (b) Structure of the cyclic ligand $[cyclo\text{-}\{As(CH_3)OAs[NC(O)CH_3]O\}_2]^{2-}$ formed by the reaction of $(CH_3AsO)_n$ with CH_3CN under these conditions [46].

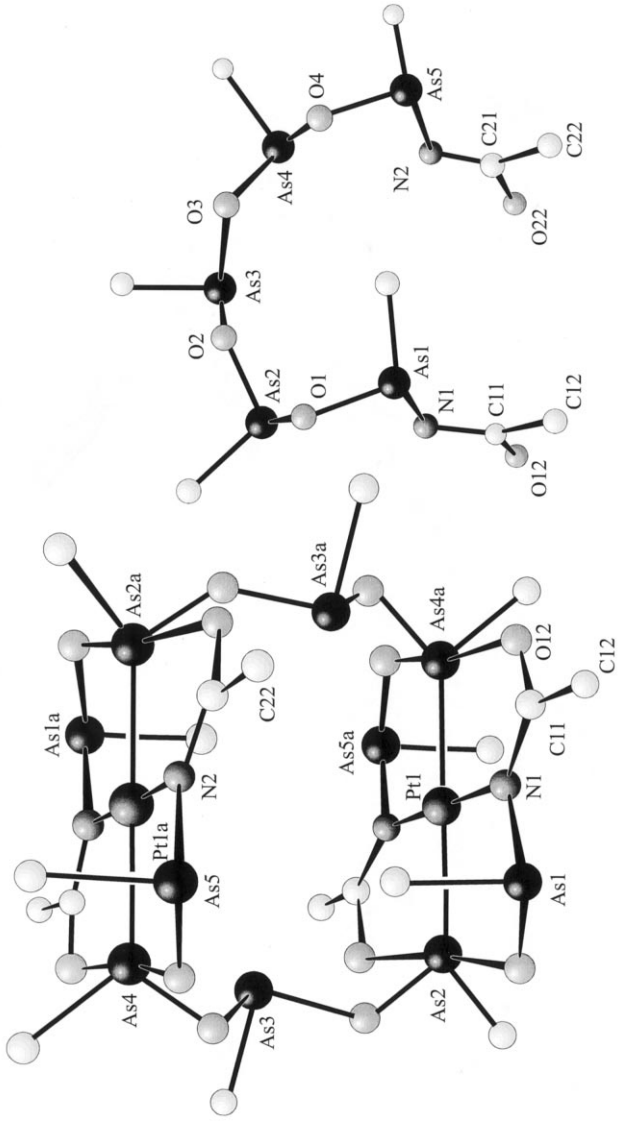

Fig. 38. (a) Molecular structure of $[Pt_2\{[CH_3C(O)N]_2As_5(CH_3)_5O_4\}_2]$, the product of the reaction between K_2PtCl_4, Ag_2CO_3 and $(CH_3AsO)_n$ in CH_3CN at 100°C. (b) Structure of the acyclic ligand $[\{CH_3C(O)N\}_2As_5(CH_3)_5O_4]^{2-}$ formed under such conditions [46].

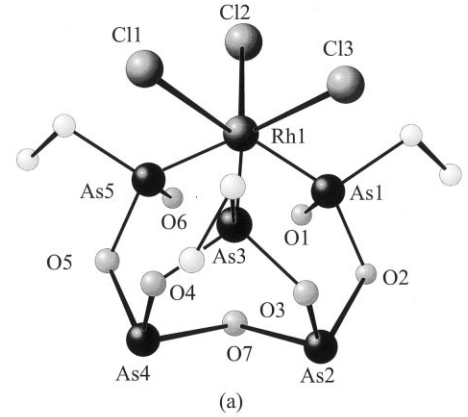

(a)

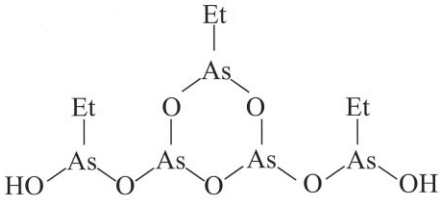

(b)

Fig. 39. (a) Molecular structure of $[RhCl_3\{As_5(C_2H_5)_2O_5(OH)_2\}]$, a minor product of the reaction of $RhCl_3{\cdot}3H_2O$ and $(C_2H_5AsO)_n$ in acetone. (b) Structure of the cyclic ligand $[As_5(C_2H_5)_2O_5(OH)_2]$ formed by hydrolysis of $(C_2H_5AsO)_n$ under these conditions [66].

rings on d(As–M) or d(S–M). For typical As–M or S–M distances in the range 2.20–2.55 Å, both κ^2As^1, As^2 and κ^2S^1, S^2 chelation in octahedral metal coordination spheres should be possible for the preferred crown conformation of tetrameric alkylcycloarsathianes. In contrast, Fig. 41 indicates that severe narrowing of the As–M–As or S–M–S angles from the ideal tetrahedral value would be required to allow the adoption of this binding mode by a Cu(I) or Ag(I) atom with a coordination number of 4. κ^2As^1, As^3 or κ^2S^1, S^3 chelation by opposite As/S atoms in the eight-membered $(AsS)_4$ ring of tetrameric alkylcycloarsathianes will, therefore, be expected in a tetrahedral metal coordination sphere.

Our recent structural studies on complexes of $(C_2H_5AsS)_4$ have confirmed these prognostications. For instance, the Cu(I) atom in $[Cu\{cyclo\text{-}(C_2H_5AsS)_4\}_2]$ CF_3SO_3 [69] is indeed coordinated in the predicted κ^2S^1, S^3 fashion by two tetrameric ethylcycloarsathiane ligands, both of which exhibit a boat-chair conformation (Fig. 42a). The Cu–S distances in the complex cation lie in the range 2.283(6)–2.340(6) Å and the endocyclic S–Cu–S angles of 112.6(2) and 114.4(2)° are close to the ideal tetrahedral value. When only the shorter Ag–S1 and Ag–S3 distances of 2.767(5) and 2.716(7) Å are taken into account, a similar κ^2S^1, S^3 chelation mode can be discerned for the $(C_2H_5AsS)_4$ ligands in $[Ag\{cyclo\text{-}(C_2H_5AsS)_4\}_2]CF_3SO_3$ [12], the

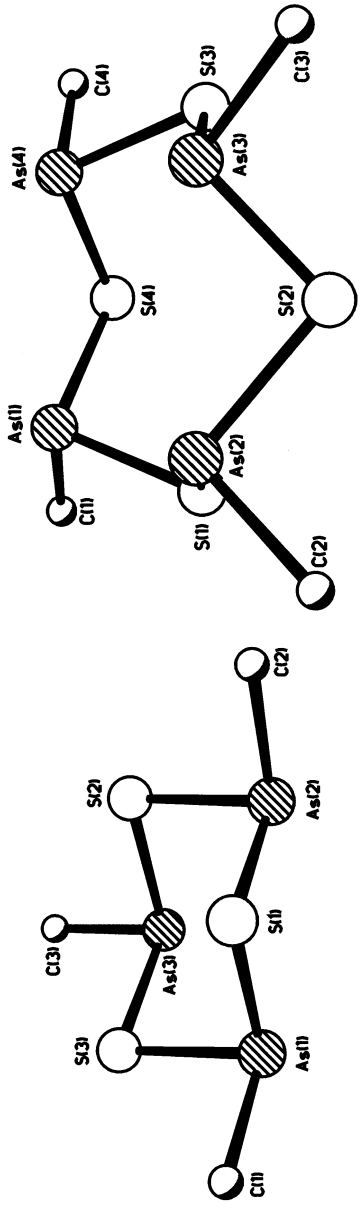

Fig. 40. Chair conformation of $(CH_3AsS)_3$ and crown conformation of $(CH_3AsS)_4$ in the solid state [18].

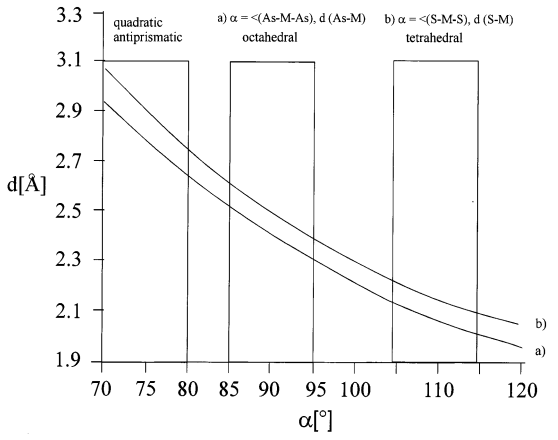

Fig. 41. Dependence of As–M–As (M = metal atom) and S–M–S angles, respectively, on (a) As–M or (b) S–M distances in four-membered chelate rings. The following average values from $(CH_3AsS)_4$ [18] and $(C_2H_5AsS)_4$ [12] were employed: d(As–S) = 2.25 Å, ∠(As–S–As) = 97.4°, ∠(S–As–S) = 102.9°.

complex cation of which displays crystallographic C_2 symmetry (Fig. 42b). However, the remaining sulphur atoms S2 and S4 of the crown shaped heterocycle also participate in the coordination sphere of the Ag(I) cation through longer Ag–S interactions of 3.328(9) and 3.218(6) Å. Whereas the As atoms in the $(AsS)_4$ ring are close to being coplanar (± 0.043 Å), larger deviations of ± 0.132 Å from a best least-squares plane are necessary for the four sulphur atoms in order to accommodate the alternating short and long As–S bonds. It is instructive to compare the coordination geometry of the silver cations in $[Ag\{cyclo\text{-}(C_2H_5AsS)_4\}_2]CF_3SO_3$ with

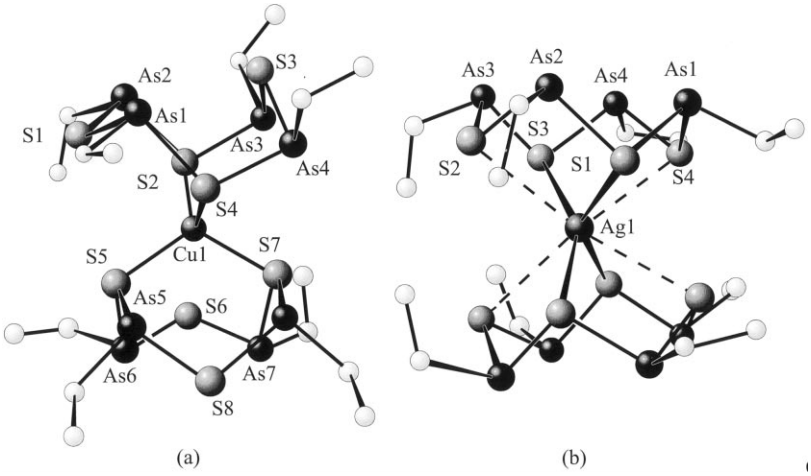

Fig. 42. Molecular structures of the cations of (a) $[Cu\{cyclo\text{-}(C_2H_5AsS)_4\}_2]CF_3SO_3$ [69] and (b) $[Ag\{cyclo\text{-}(C_2H_5AsS)_4\}_2]CF_3SO_3$ [12].

that of an idealised quadratic antiprism. If one defines the centres of the S_4 planes of the cycloarsathiane rings as respectively Pl and Pl′, then the observed torsion angles S–Pl–Pl′–S′ exhibit alternating average values of 41.6(5) and −48.4(4)°, i.e. in comparison to the expected value of 45° for a quadratic antiprism, the coordination polyhedron in the complex cation displays an 8% distortion towards a cube. All four independent S–Ag–Pl angles lie in the narrow range 52.7–56.0° and are, therefore, relatively close to the characteristic α value of 57° found in transition metal complexes ML_8 [38]. A more pronounced longitudinal distortion is observed in the ethylcycloarsoxane complex $[Na\{cyclo\text{-}(C_2H_5AsO)_4\}_2]^+$, with its average α value of only 47.2° [32].

Both of the above complexes contain the tetrameric ligand $(C_2H_5AsS)_4$, as do $[cyclo\text{-}(C_2H_5AsS)_4]\cdot 2SbBr_3$ [12] and $[RuCl_2\{cyclo\text{-}(C_2H_5AsS)_4\}(Ph_3P)]$ [70]. Despite its presence in solution [12], no examples are known in which the competitive cyclotrimer $(C_2H_5AsS)_3$ is stabilised in the coordination sphere of a metal atom. Interestingly [9]aneS_3 has been found to be capable of enforcing an elongated octahedral geometry with average chelating S–Ag–S′ angles of 80° on the Ag(I) cation in $[Ag([9]aneS_3)_2]^+$ [71]. An analogous facial $\kappa^3 S$ coordination mode has also been established for this macrocyclic thioether in [9]ane$S_3\cdot SbI_3$ [72], whose chelating S–Ag–S′ angles in the range 74.0–74.8° are even narrower than those in $[Ag([9]aneS_3)_2]^+$. In contrast, only one of the four potential S donor atoms in $(C_2H_5AsS)_4$ is involved in antimony coordination in polymeric $[cyclo\text{-}(C_2H_5AsS)_4]\cdot 2SbBr_3$ [12]. An explanation for the reluctance of $(C_2H_5AsS)_3$ to participate in complex formation may be sought in the shortness of its intramolecular S···S distances, which would lead to unfavourably small S–Ag–S or S–Sb–S angles of bite in hypothetical compounds such as $[Ag\{cyclo\text{-}(C_2H_5AsS)_3\}_2]\ CF_3SO_3$ or $[cyclo\text{-}(C_2H_5AsS)_3]\cdot SbBr_3$.

The molecular structure of $[RuCl_2\{cyclo\text{-}(C_2H_5AsS)_4\}(Ph_3P)]$ [70] is depicted in Fig. 43. This OC-6-43 stereoisomer, in which $(C_2H_5AsS)_4$ exhibits a facial $\kappa^3 As$ coordination mode, may be isolated as a red crystalline product by covering an equimolar $[RuCl_2(Ph_3P)_3]/(C_2H_5AsS)_n$ $(n=4)$ reaction mixture in CH_2Cl_2 with hexane at room temperature. However a ^{31}P-NMR spectrum of the reaction solution after 12 h contains no less than 11 resonances in the range $\delta = 18.91$–64.06, thereby indicating the presence of further geometrical or linkage isomers [e.g. $\kappa^3 As^1$, S^2, As^4 or $\kappa^3 As^1$, As^2, S^3]. The isolated complex (Fig. 43) confirms that $\kappa^2 As^1$, As^2 four-membered chelate rings are possible for $(C_2H_5AsS)_4$ in an octahedral coordination sphere.

3.3. Metal-assisted assembly of chain and macrocyclic As–S ligands

DiMaio and Rheingold isolated the molybdenum carbonyl complex $[Mo(CO)_3\{(CH_3)_6As_6S_3\}]$, with a nine-membered partially sulphurated aresenic ring, as a by-product of the reaction between $(CH_3As)_5$ and S_8 in the presence of toluene at 125°C [18]. $Mo(CO)_6$ mediation apparently facilitates the formation of a mixture of the cyclic oligomers $(CH_3AsS)_3$ and $(CH_3AsS)_4$ as the major products of this reaction. The same authors also reported the preparation of a novel

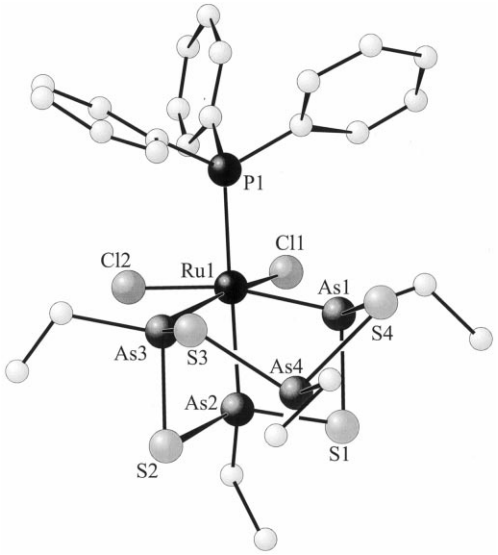

Fig. 43. Molecular structure of $[RuCl_2\{cyclo\text{-}(C_2H_5AsS)_4\}(Ph_3P)]$ [70].

tripledecker sandwich $[(CpMo)_2(\mu\text{-}As_3)(\mu\text{-}AsS)]$ by treating $[\{MoCp(CO)_3\}_2]$ with $(CH_3AsS)_n$ in toluene in a Carius tube at the same temperature [18]. However, no evidence was found for the formation of coordinated intact $(CH_3AsS)_n$ with either the $Mo(CO)_3$ or MoCp fragment, suggesting that a metal-assisted ring expansion may well be less facile for cycloarsathianes than for cycloarsoxanes and that As–S bond cleavage followed by reassembly into new ligands in the coordination sphere of transition metals can be expected at elevated temperature.

A further example of such a metal-mediated reassembly process is provided by the reaction of $[ReBr(CO)_5]$ with $(C_2H_5AsS)_n$ in toluene at reflux, which leads to the formation of the novel chain anion $[(C_2H_5)_4As_4S_5]^{2-}$ as a bridging hexadentate ligand in the dinuclear complex $[\{Re(CO)_3\}_2\{\mu\text{-}(C_2H_5)_4As_4S_5\}]$ [70]. A possible reaction mechanism would involve an initial bidentate coordination of each of the Re atoms by alternating As atoms of an intact cyclotetramer $(C_2H_5AsS)_4$, followed by nucleophilic attack of S^{2-} on As(1) or As(4) in Fig. 44. The driving force for the formation of this dirhenium compound is presumably provided by the stability of the resulting Re–S(thiolate) bonds. Kekia and Rheingold have very recently prepared the metallacycle complexes $[Cp_2M(-SCH_3AsSCH_3AsS-)]$ (M = Ti, Zr, Hf) and $[Cp_2Zr(-SCH_3AsS-)]$ with analogous though shorter chain anions by reacting the sodium-reduced form of methylcycloarsathiane with Group 4 metallocene dichlorides [73].

Metal-mediated assembly of novel macrocyclic As–S ligands has been studied in our research group [70]. Reaction of MCl_3 (M = Ru, Os) with $(C_2H_5AsS)_n$ in toluene in a Carius tube at respectively 105°C (24 h) and 140°C (70 h) leads to formation of $[M\{cyclo\text{-}(C_2H_5)_6As_8S_{10}\}]$, whose 16-membered hexadentate As–S

ring system is depicted in Fig. 45. Bond angles in the range 80.5(2)–101.2(1)° are observed for the distorted octahedral coordination sphere of the central osmium atom in [Os{*cyclo*-$(C_2H_5)_6As_8S_{10}$}]. The reduction of M(III) to M(II) (M = Ru, Os) required for the preparation of these isostructural complexes poses the question as to the nature of the accompanying oxidation. It seems reasonable to assume that S–S bond formation will be involved and this hypothesis is, at least, partially substantiated by the isolation of a second Ru(II) complex, [Ru{*cyclo*-$(C_2H_5)_4As_6S_{10}$}] (Fig. 46) by employment of a longer reaction time (70 h) at higher temperature (140°C). An analogous Os(II) complex could not be isolated, even at considerably higher temperature (200°C). The novel 14-membered ring of the hexadentate ligand $[(C_2H_5)_4As_6S_{10}]^{2-}$ exhibits crystallographic C_{2h} symmetry and contains two S–S bonds. The thiolate sulphur atoms S1/S1a are now sited *trans* to one another and the novel macrocycle is effectively perfectly dimensioned for octahedral coordination of Ru(II), as evidenced by the similar Ru–As and Ru–S

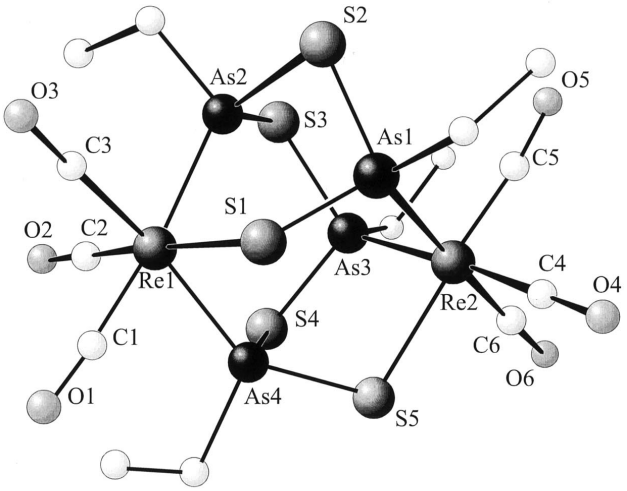

(a)

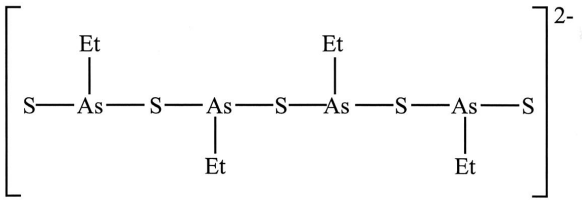

(b)

Fig. 44. Molecular structure of [{$Re(CO)_3$}$_2${μ-$(C_2H_5)_4As_4S_5$}] [70].

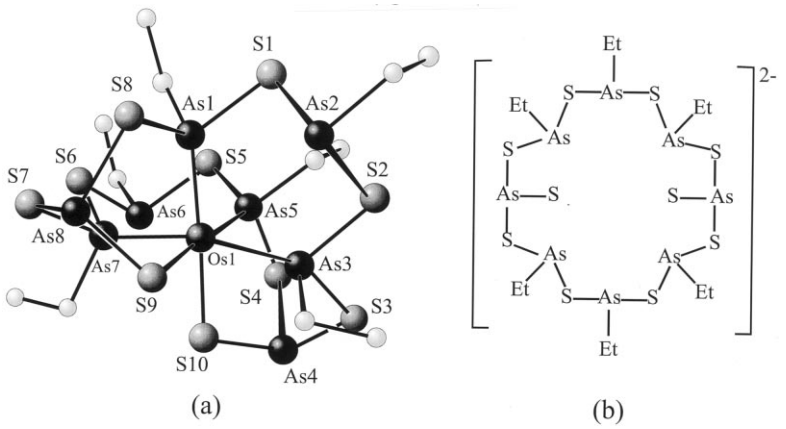

Fig. 45. (a) Molecular structure of $[Os\{cyclo\text{-}(C_2H_5)_6As_8S_{10}\}]$ prepared by reaction of $OsCl_3$ and $(C_2H_5AsS)_n$ in toluene for 70 h at 140°C. (b) Structure of the macrocyclic ligand $[(C_2H_5)_6As_8S_{10}]^{2-}$ formed under these conditions [70].

distances [2.391(2), 2.378(6) Å] and the very minor deviations [88.7(1)–91.3(1)°] from the ideal octahedral angle. This finding is in accordance with the assumed increased thermodynamic stability of $[Ru\{cyclo\text{-}(C_2H_5)_4As_6S_{10}\}]$ in comparison to $[Ru\{cyclo\text{-}(C_2H_5)_6As_8S_{10}\}]$, which can be presumed to be an intermediate product on the reaction pathway to the former complex.

4. Summary and outlook

Alkylcycloarsoxanes $(RAsO)_n$ ($R = CH_3$, C_2H_5) are multidentate ligands capable of coordinating either hard or soft metal fragments in respectively in $\kappa^n O$ or κAs–$\kappa^4 As$ modes. They are characterised by their unique ability to undergo metal-mediated ring expansion to $n = 4$, 5, 6 or 8 and by their remarkable conformational flexibility. Furthermore, our recent studies presented in this review article indicate that their cyclotetramers $(RAsO)_4$ exhibit considerable potential as $\kappa^2 As^1$, As^3 linking macrocycles for the construction of novel multifunctional coordination networks with an ability to host a variety of guests such as alkali cations or polar organic molecules (e.g. CH_3OH, CH_3CN, C_6H_5CN). The combination of these ion ligating $(AsO)_4$ heterocycles and rigid aromatic ligands as spacers between metal coordination polyhedra in flexible porous sheet or framework polymers is particularly promising.

Intact tetrameric alkylcycloarsathianes $(RAsS)_4$ can be stabilised in the coordination sphere of coinage or transition metals under mild conditions and should be capable of enforcing unusual coordination geometries, e.g. the quadratic antiprismatic environment of the silver(I) cations in $[Ag\{cyclo\text{-}(C_2H_5AsS)_4\}_2]^+$. At elevated

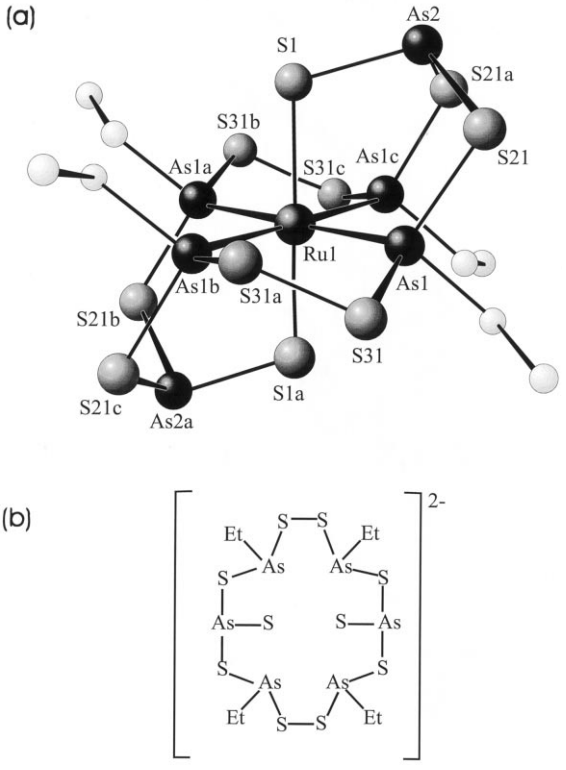

Fig. 46. (a) Molecular structure of $[Ru\{cyclo\text{-}(C_2H_5)_4As_6S_{10}\}]$ prepared by reaction of $RuCl_3$ and $(C_2H_5AsS)_n$ for 70 h at 140°C. (b) Structure of the macrocyclic ligand $[(C_2H_5)_4As_6S_{10})]^{2-}$ assembled in the octahedral Ru(II) coordination sphere [70].

temperatures, As–S bond cleavage and metal-assisted reassembly can afford novel chainlike and macrocyclic ligands that are tailored for the coordination of the structure directing metal atom.

After submission of this article, Kekia and Rheingold [74] have reported the preparation of $[Cr\{cyclo\text{-}(CH_3AsS)_4\}(CO)_5]$, $[Cr\{cyclo\text{-}(CH_3AsS)_5\}(CO)_3]$ and $[W\{cyclo\text{-}(CH_3AsS)_6\}(CO)_3]$ by photolysis of $(CH_3AsS)_n$ with Group 6 carbonyls $M(CO)_6$ [M = Cr, W] in THF.

Acknowledgements

The authors would particularly like to express their thanks to Dr. Thomas Häusler whose pioneering studies (1992–1995) on the coordination preperties of $(C_2H_5AsO)_n$ and $(C_2H_5AsS)_n$ are discussed in detail in this review article.

References

[1] A. von Baeyer, Ann. Chem. 107 (1858) 279.
[2] (a) A. Michaelis, Chem. Ber. 10 (1877) 622. (b) W. LaCoste, A. Michaelis, Ann. Chem. 201 (1880) 200.
[3] C. Schulte, Chem. Ber. 15 (1882) 1952.
[4] (a) C. Voegtlin, J.W. Thompson, J. Pharmacol. Exp. Ther. 20 (1922) 85. (b) C. Voegtlin, H.W. Smith, J. Pharmacol. Exp. Ther. 16 (1921) 199, 449.
[5] F.F. Blicke, F.D. Smith, J. Am. Chem. Soc. 52 (1930) 2946.
[6] H.C. Marsmann, J.R. Van Wazer, J. Am. Chem. Soc. 92 (1970) 3969.
[7] M. Durand, J.-P. Laurent, J. Organomet. Chem. 77 (1974) 225.
[8] W.S. Sheldrick, T. Häusler, Z. Naturforsch. Teil B 48 (1993) 1069.
[9] A.-J. DiMaio, A.L. Rheingold, Organometallics 10 (1991) 3764.
[10] I.M. Müller, Diploma Thesis, Ruhr-Universität Bochum, 1994.
[11] A.M. Arif, A.H. Cowley, M. Pakulski, J. Chem. Soc. Chem. Commun. (1987) 165.
[12] T. Häusler, W.S. Sheldrick, Z. Naturforsch. Teil B 49 (1994) 1215.
[13] J.T. Shore, W.T. Pennington, A.W. Cordes, Acta Crystallogr. Sect. C 44 (1988) 1831.
[14] G. Bergerhoff, H. Namgung, Z. Kristallogr. 150 (1979) 209.
[15] A.E. Kretov, A. Ya. Berlin, J. Gen. Chem. USSR (Engl. Transl.) 1 (1931) 411.
[16] L. Anschütz, H. Wirth, Chem. Ber. 89 (1956) 1530.
[17] R.A. Zingaro, R.E. McGlothlin, R.M. Hedges, Trans. Faraday Soc. 59 (1963) 798.
[18] A.-J. DiMaio, A.L. Rheingold, Inorg. Chem. 29 (1990) 798.
[19] A.L. Rheingold, A.-J. DiMaio, Organometallics 5 (1986) 393.
[20] A. Tzschach, J. Heinicke, in: Arsenheterocyclen, VEB Deutscher Verlag für Grundstoffindustrie, Leipzig, 1978, p. 85.
[21] D.B. Sowerby, in: I. Haiduc, D.B. Sowerby (Eds.), The Chemistry of Inorganic Homo- and Heterocycles, Part 2, Academic Press, London, 1987, p. 718.
[22] W. Steinkopf, W. Mieg, Chem. Ber. 53 (1920) 1013.
[23] A. McKenzie, J.K. Wood, J. Chem. Soc. 117 (1920) 406.
[24] V. Auger, Compt. Rend. Acad. Sci. Paris 137 (1903) 925.
[25] R.L. Barker, E. Booth, W.E. Jones, A.F. Millidge, F.N. Woodward, J. Soc. Chem. Ind. (London) 68 (1949) 289.
[26] A.W. Palmer, W.M. Dehn, Chem. Ber. 34 (1901) 3594.
[27] G. Petit, Ann. Chim. 16 (1941) 5.
[28] J.B. Hendrickson, J. Am. Chem. Soc. 89 (1967) 7036.
[29] (a) R.M. Bozarth, J. Am. Chem. Soc. 45 (1923) 1621. (b) L.R. Maxwell, S.B. Hendricks, L.S. Deming, J. Chem. Phys. 5 (1937) 626.
[30] J. Ellerman, L. Brehm, E. Lindner, W. Hiller, R. Fawzi, F.L. Dickert, M. Waidhas, J. Chem. Soc. Dalton Trans. (1986) 997.
[31] J. Kopf, K. von Deuten, G. Klar, Inorg. Chim. Acta 38 (1980) 67.
[32] I.M. Müller, Dissertation, Ruhr-Universität Bochum, 1997.
[33] W.S. Sheldrick, T. Häusler, Z. Anorg. Allg. Chem. 619 (1993) 1984.
[34] T. Häusler, W.S. Sheldrick, Chem. Ber. 130 (1997) 371.
[35] R.D. Shannon, C.T. Prewitt, Acta Crystallogr. Sect. B 25 (1969) 925.
[36] F.P. Boer, M.A. Neumann, F.P. van Remoortere, E.C. Steiner, Inorg. Chem. 13 (1974) 2826.
[37] P.R. Mallison, M.R. Truter, J. Chem. Soc. Perkin Trans. (1972) 1818.
[38] D.L. Kepert, Inorganic Stereochemistry, Springer-Verlag, Berlin, 1982, p. 153.
[39] E.W. Abel, I.S. Butler, Trans. Faraday Soc. 63 (1967) 45.
[40] I.M. Müller, W.S. Sheldrick, Z. Anorg. Allg. Chem. 623 (1997) 1399.
[41] I.M. Müller, W.S. Sheldrick, Z. Naturforsch. Teil B 52 (1997) 951.
[42] W.S. Sheldrick, T. Häusler, Z. Anorg. Allg. Chem. 620 (1994) 334.
[43] I.M. Müller, T. Röttgers, W.S. Sheldrick, J. Chem. Soc. Chem. Commun. (1998) 823.
[44] A. Whitaker, J.W. Jeffrey, Acta Crystallogr. 23 (1967) 977.

[45] T. Häusler, W.S. Sheldrick, Z. Naturforsch. Sect. B 52 (1997) 679.
[46] I.M. Müller, W.S. Sheldrick, Eur. J. Inorg. Chem., in press.
[47] B.F. Hoskins, R. Robson, J. Am. Chem. Soc. 112 (1990) 1546.
[48] R. Robson, B.F. Abrahams, S.R. Batten, R.W. Grable, B.F. Hoskins, J. Liu, Supramolecular Architecture, ACS, Washington, DC, 1992, Ch. 19.
[49] M.J. Zaworotko, Chem. Soc. Rev. 23 (1994) 283.
[50] C. Janiak, Angew. Chem. Int. Ed. Engl. 36 (1997) 1431.
[51] J.R. Blake, N.R. Champness, W. Levason, C. Reid, Inorg. Chem. 35 (1996) 4432.
[52] A.J. Blake, D. Collins, R.O. Gould, C. Reid, M. Schröder, J. Chem. Soc. Dalton Trans. (1993) 521.
[53] M. Munakata, L.P. Wu, M. Yamamoto, T. Kuroda-Sowa, M. Maekawa, J. Chem. Soc. Dalton Trans. (1995) 3215.
[54] A.J. Blake, W.-S. Li, V. Lippolis, M. Schröder, J. Chem. Soc. Chem. Commun. (1997) 1943.
[55] H. van Bekkum, E.M. Flanigen, J.C. Jansen (Eds.), Introduction to Zeolite Science and Practice, Elsevier, Amsterdam, 1991.
[56] G.A. Ozin, Supramol. Chem. 6 (1995) 125.
[57] W.S. Sheldrick, M. Wachhold, Angew. Chem. Int. Ed. Engl. 36 (1997) 206.
[58] T. Iwamoto, S. Nishikiori, T. Kitazawa, H. Yuge, J. Chem. Soc. Dalton Trans. (1997) 4127.
[59] B.F. Abrahams, S.R. Batten, H. Hamit, B.F. Hoskins, R. Robson, J. Chem. Soc. Chem. Commun. (1996) 1313.
[60] K.A. Hirsch, D. Venkataraman, S.R. Wilson, J.S. Moore, S. Le, J. Chem. Soc. Chem. Commun. (1995) 2199.
[61] L. Carlucci, G. Ciani, D.M. Proserpio, A. Sironi, J. Chem. Soc. Chem. Commun. (1996) 1393.
[62] J.A. Swift, V.A. Russell, M.D. Ward, Adv. Mater. 9 (1997) 1183.
[63] I.M. Müller, T. Röttgers, W.S. Sheldrick, 1998, unpublished results.
[64] P. Behrens, G.D. Stucky, in: J.L. Atwood, D.D. MacNoil, J.E.D. Davies, F. Vögtle, G. Alberti, T. Bein (Eds.), Comprehensive Supramolecular Chemistry, vol. 7, Pergamon Press, Oxford, 1996, Ch. 25.
[65] J.S. Bradshaw, R.M. Izatt, Acc. Chem. Res. 30 (1997) 338.
[66] T. Häusler, Dissertation, Ruhr-Universität Bochum, 1995.
[67] F.F. Blicke, L.D. Powers, J. Am. Chem. Soc. 55 (1933) 1161.
[68] L. Anschütz, H. Wirth, Naturwisschenschaften 43 (1956) 59.
[69] T. Häusler, W.S. Sheldrick, unpublished results.
[70] T. Häusler, W.S. Sheldrick, Chem. Ber. 129 (1996) 131.
[71] P.J. Blower, J.A. Clarkson, S.C. Rawle, et al., Inorg. Chem. 28 (1989) 4040.
[72] S. Pohl, D. Haase, M. Peters, Z. Anorg. Allg. Chem. 619 (1993) 727.
[73] O.M. Kekia, A.L. Rheingold, Organometallics 16 (1997) 5142.
[74] O.M. Kekia, A.L. Rheingold, Organometallics 17 (1998) 726.